remote sensing

MDPI

Article

Spatiotemporal Changes and Driving Analysis of Ecological Environmental Quality along the Qinghai–Tibet Railway Using Google Earth Engine—A Case Study Covering Xining to Jianghe Stations

Fengli Zou [1,*], Qingwu Hu [2], Yichuan Liu [3], Haidong Li [4], Xujie Zhang [2] and Yuqi Liu [5]

[1] School of Geography and Tourism, Qufu Normal University, Rizhao 276800, China
[2] School of Remote Sensing and Information Engineering, Wuhan University, Wuhan 430079, China; huqw@whu.edu.cn (Q.H.); ac_zxj@whu.edu.cn (X.Z.)
[3] Henan Provincial Meteorological Disaster Defense Technology Center, Zhengzhou 450003, China; sxthpf@163.com
[4] Nanjing Institute of Environmental Sciences, Ministry of Ecology and Environment, Nanjing 210042, China; lihd2020@163.com
[5] Map Institute of Guangdong Province, Guangzhou 510075, China; 15225888480@163.com
* Correspondence: zoufengli2022@163.com

Abstract: The Qinghai–Tibet Railway is located in the most fragile and sensitive terrestrial ecosystem of the Qinghai–Tibet Plateau in China, and once the ecological environment is damaged, it is difficult to restore. This study, based on the Google Earth Engine platform, focuses on the section of the Qinghai–Tibet Railway from Xining to Jianghe. It utilizes Landsat series satellite imagery data from 1986 to 2020 to calculate the Remote Sensing Ecological Index (RSEI). This approach enables large-scale and long-term dynamic monitoring, analysis, and assessment of the ecological changes along the Qinghai–Tibet Railway corridor. The results indicate that (1) the average RSEI of the study area increased from 0.37 in 1986 to 0.53 in 2020, showing an overall trend of improvement. The ecological environment quality is mainly categorized as medium and good. (2) The quality of the ecological environment in the areas along the railway experienced fluctuations during different periods of railway construction and operation. From 1986 to 1994, after the first phase of the railway opened, the overall ecological environment showed a relative decline in quality. From 1994 to 2002, the ecological quality of 60% of the region saw slight improvements. During the extension construction of the second phase of the railway from 2002 to 2007, the regional ecology fluctuated again. However, from 2013 to 2020, during the operational period, a stable recovery trend was observed in the ecological environment. (3) The ecological environment in the study area is influenced by multiple factors. Different railway station areas exhibit strong spatial heterogeneity. The impact of single factors is significant, with the existence of spatial stratification and enhanced interactions among multiple factors. The strongest interactive effects are observed between land use types, the intensity of human activities, and temperature.

Keywords: the Qinghai–Tibet Railway; remote sensing; ecological environment quality

Citation: Zou, F.; Hu, Q.; Liu, Y.; Li, H.; Zhang, X.; Liu, Y. Spatiotemporal Changes and Driving Analysis of Ecological Environmental Quality along the Qinghai–Tibet Railway Using Google Earth Engine—A Case Study Covering Xining to Jianghe Stations. *Remote Sens.* **2024**, *16*, 951. https://doi.org/10.3390/rs16060951

Academic Editors: Chengye Zhang, Huazhong Ren and Yuanheng Sun

Received: 20 January 2024
Revised: 29 February 2024
Accepted: 2 March 2024
Published: 8 March 2024

1. Introduction

The Qinghai–Tibet Plateau, with its low latitude and high altitude, is known as the "Third Pole" of the Earth. It possesses a unique alpine ecosystem. The ecological environment is extremely fragile and highly sensitive to global climate change and human activities. It is also referred to as a driver and amplifier of global climate change [1]. Restricted by various natural conditions such as cold, drought, and high altitude, few species are able to survive on the Qinghai–Tibet Plateau. The various types of flora and fauna present there have very short life cycles. In its entire ecosystem, the overall biomass

is low, the food chains formed are relatively simple, and the rate of material and energy conversion is extremely slow [2]. Therefore, if the ecological environment of the Qinghai–Tibet Plateau is damaged, it would be very difficult to restore, and it might even trigger serious environmental problems [3].

The Qinghai–Tibet Railway, along with the South–North Water Transfer Project, the West–East Gas Pipeline, and the West-to-East Electricity Transmission, is collectively known as the "Four Great New Projects" of New China. The construction of the railway is of great significance for accelerating the economic and social development of the western regions, especially the Tibet area [4]. Geological issues associated with large-scale engineering projects have received widespread attention. For instance, in the construction of the Qinghai–Tibet Railway, factors such as the use of engineering land [5], disposal of excavated soil [6], construction access roads [7], and pollution from inorganic substances and heavy metals [8,9] have formed ecological disturbance corridors. This leads to changes in sun exposure angles [10], hydrothermal conditions [11,12], surface runoff [13], and permafrost structures [14], thereby interrupting ecological water usage [15], damaging soil water retention capacity [16], and thus inducing ecological and environmental problems. Therefore, the Qinghai–Tibet Railway is a high-altitude railway in the world with extremely high construction, maintenance, and operational challenges. It serves as a rational area for studying the impact of large-scale human engineering activities on ecosystems [17].

After its opening, the Qinghai–Tibet Railway became a crucial engineering project and transportation corridor connecting the Chinese hinterland with the Qinghai–Tibet Plateau. It broke the transportation bottleneck that hindered the economic and social development of the plateau. It plays a vital role in the economic development and social stability of the Qinghai–Tibet region, significantly accelerating the development of tourism in the surrounding areas [18]. Particularly, it has promoted the economic and population growth of cities along the railway, such as Xining, the largest city along the Qinghai–Tibet Railway, which has developed into a regional modernized city with a population of over 1 million on the Qinghai–Tibet Plateau [19].

In recent years, with the continuous deepening of ecological construction concepts, an increasing number of scholars both domestically and internationally have begun to focus on the impact of the construction and development of transportation infrastructure on regional ecological environments [20]. Due to the fragility and sensitivity of the ecosystems along the Qinghai–Tibet Railway, the impact of the railway on ecological changes has always been a key research topic [21]. However, current studies on the ecological environment changes along the Qinghai–Tibet Railway often concentrate on single aspects such as vegetation, meteorological factors, or land use types as main characteristic indicators. A significant amount of research, taking alpine vegetation as a starting point, investigates changes in vegetation coverage, net primary productivity (NPP) [22], and biomass along the railway. For instance, according to Chen Hui [22], based on field survey data from August 2001 to 2002, it is believed that the construction of highways and railways directly cuts through the ecosystems along their routes. This results in a more fragmented landscape and consequently a decrease in the annual net primary productivity and biomass of vegetation. Ding [23,24] studied the changes in vegetation cover along the Qinghai–Tibet Highway and the Golmud–Lhasa section of the railway prior to their construction (1981–2001). They believe that over the span of 20 years, the vegetation cover in the study area generally tended towards stability. Zhang [25] believed that the construction of the Golmud–Lhasa section of the Qinghai–Tibet Railway involved a massive amount of earth and stone works, which could potentially cause a certain degree of damage to the surface vegetation. As a result, this might lead to land desertification, soil erosion, wetland shrinkage, and other issues. Luo [26] studied the impact of climate change and human activities on the alpine vegetation and permafrost along the Qinghai–Tibet Engineering Corridor (Golmud–Lhasa section) from 1981 to 2010. The study indicates that climatic warming and humidification have a promoting effect on vegetation ecology, while construction projects have led to the degradation of alpine vegetation and other issues. Overall, the monitoring of the ecological

environment along railway lines focuses predominantly on studies responding to changes in vegetation ecology, and there is a lack of comprehensive research on the response of multiple natural environmental factors to changes in the quality of the regional ecological environment.

This paper focuses on studying the changes in ecological environment quality along the Qinghai–Tibet Railway. Ecological environment quality assessment is a crucial means for quantitatively evaluating the quality and impact of the regional ecological environment. It forms an important basis for formulating plans for regional socioeconomic sustainable development and strategies for ecological environment protection. Satellite remote sensing technology, with its advantages of wide-area, real-time, rapid, and periodic repeated observations, is widely used in ecological environment quality monitoring research [27–29]. Various remote sensing indices have been proposed by scholars, and a series of remote sensing monitoring and evaluation studies have been carried out on urban areas [30], land [31], and vegetation [32]. Compared to traditional single-index ecological evaluations, the RSEI proposed by Xu [33], which is entirely based on remote sensing information, integrates a variety of natural environmental indicators. This approach allows for a more scientific and comprehensive assessment of regional ecological environment quality [34]. The RSEI synthesizes four ecological indicators—greenness, wetness, heat, and dryness—without using parameters to comprehensively reflect the quality of the regional ecological environment. Numerous studies have shown that greenness, wetness, heat, and dryness are the most important characteristic variables among many natural factors that reflect ecological quality [35,36]. RSEI has proven to be effective in assessing regional ecological environmental quality and has been widely applied [30,37,38]. However, its application to larger areas still faces challenges due to the vast amount of data required and the consequent complexity and enormity of model computations.

The Google Earth Engine (GEE) platform is equipped with an extensive archive of historical remote sensing imagery and is also a high-performance cloud service platform capable of parallel computing [39]. GEE has been widely used in data fusion [40], multi-temporal image classification [41], change detection [42], and monitoring of land cover and land use dynamics [43]. The research, based on the Google Earth Engine (GEE) platform, utilized Landsat TM/OLI imagery data from 1986 to 2020. By constructing cloud-free images through minimum cloud amount synthesis and combining sub-indicators, a remote sensing ecological index model was built. The study involved large-scale, long-term dynamic monitoring and analysis of the ecological environment quality along the Qinghai–Tibet Railway from 1986 to 2020, focusing on different railway construction times and the spatial aspects of various train stations. Using the geodetector model, the study explored the spatial heterogeneity of the railway's ecological environment and its driving factors. The aim was to reveal the spatiotemporal characteristics and driving mechanisms of ecological environment quality changes in ecologically sensitive areas under the backdrop of large-scale human engineering activities. Timely and accurate mastery of the status and trends of ecological environment quality will provide targeted scientific basis and technical support for the formulation of ecological protection policies and the assessment of the effectiveness of ecological projects in the Qinghai–Tibet Plateau region.

2. Materials and Methods

2.1. Study Area

The Qinghai–Tibet Railway is the first railway connecting the hinterland of Tibet, starting from Xining in Qinghai Province to Lhasa in the Tibet Autonomous Region. Along the route, there are a total of 85 stations, and the railway spans a total length of 1956 km (Figure 1). The Qinghai–Tibet Railway includes the section from Xining to the Nanshankou of Golmud, which is 814 km long and was completed in 1979 and put into operation in 1984. The section from Nanshankou in Golmud to Lhasa starts from Golmud City in Qinghai Province and extends west to Lhasa City in the Tibet Autonomous Region, spanning a total length of 1142 km. Of this, 1107 km were newly constructed. This section was fully

operational in 2006. From 2007 to 2011, the double-tracking of the railway from Xining to Golmud was completed.

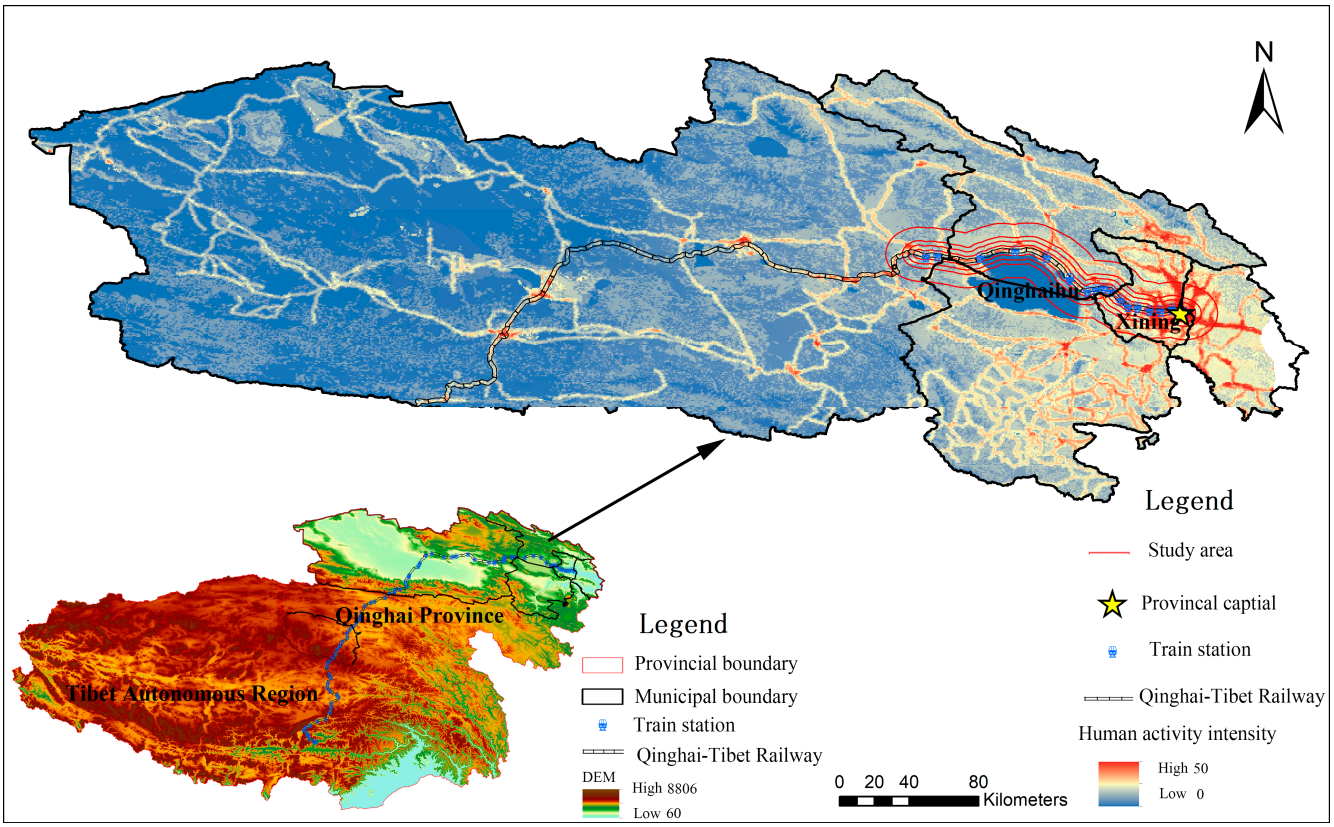

Figure 1. The Qinghai–Tibet Railway and basic geographical location map of the study area.

The Qinghai–Tibet Railway serves as the primary transportation hub connecting the Qinghai–Tibet Plateau region with other areas. Along its route, the railway connects major towns and cities in the plateau region. Among them, Xining, where the Xining station is located, has developed into the largest and most modernized city in the Qinghai–Tibet Plateau area. Near the Qinghai Lake station is the Qinghai Lake National Nature Reserve. Qinghai Lake, located in this region, is one of the highest lakes in the world and a typical representative of the high plateau inland lake wetland type. The area around the lake has developed a unique cultural identity that is characteristic of Tibetan culture. Along the transportation route, important bases for animal husbandry, tourism, and industry have formed in the Qinghai–Tibet Plateau region. The Qinghai–Tibet Railway runs parallel to the Qinghai–Tibet Highway. The closest distance between them is designed to be 2 km, while the farthest distance is 16 km [1]. Considering the above factors and in conjunction with the experiments on vegetation ecological sensitivity conducted in the experimental area of this study, this paper selects the Xining and Jianghe station sites as the central points of the buffer zone. The buffer radius is 30 km on both sides of the railway line. The study area for this paper is approximately 300 km by 60 km, starting from Xining West Station and ending at Tianpeng Station (Figure 1). The time periods of 1986–1994, 1994–2007, 2007–2013, and 2013–2020 have been set as the research sequences for studying the different construction and operational phases of the Qinghai–Tibet Railway in this study.

2.2. Data Sources

2.2.1. Landsat Data and Preprocessing

In this paper, the basic Landsat data used include Landsat 5 (TM), Landsat 7 (ETM+), and Landsat 8 (OLI). Specifically, the data are from the Landsat Level 2, Collection 2 surface

reflectance and products. These data have a spatial resolution of 30 m and a temporal resolution of 16 days. In this study, surface reflectance is radiometrically corrected to obtain TOA reflectance products. During the calculation of TOA products, the maximum cloud content for the cloud control layer is dynamically selected based on the actual cloud cover in the test area. The maximum cloud content in the TOA products calculated for this study is consistently less than 15%. Subsequently, the TOA products obtained are used as supplementary data for the missing areas in the SR products, synthesizing a comprehensive surface reflectance product with a total cloud content of less than 15%. The acquisition and processing of the source data are entirely conducted on the GEE platform.

2.2.2. Other Data and Preprocessing

The data used for calculating human activity intensity include population density, land use, cattle and sheep density, night-time lighting, railways, roads, and cattle and sheep meat production data. Among these, the population density and land use data are provided by the GEE platform, with population density data sourced from https://ngdc.noaa.gov/eog/dmsp/downloadV4composites.html (accessed on 15 January 2023) and land use data from MODIS/006/MCD12Q1. The cattle and sheep meat production data are obtained from the National Bureau of Statistics website (http://www.stats.gov.cn/ (accessed on 14 January 2023). Cattle and sheep density data are sourced from the Food and Agriculture Organization (FAO) of the United Nations' Global Geographical Information System website. Night-time lighting data are acquired from the National Oceanic and Atmospheric Administration (NOAA) website and the GEE platform. Railway and road data are obtained from OpenStreetMap and the NASA Earth Observing System Data and Information System website. In this paper, after uniformly preprocessing the aforementioned data, a human activity intensity dataset is constructed using the human footprint synthesis method on the GEE platform.

The temperature and precipitation observation data for meteorological stations along the Qinghai–Tibet Railway from 1986 to 2020 used in this paper are sourced from the National Meteorological Administration data website. After spatial interpolation calculations, the meteorological dataset used for this study was obtained.

The vector data used in the paper are sourced from the "National Basic Geographic Information System 1:4 million data". The 90 m spatial-resolution DEM data and the 30 m land use (Globeland30) data used in the study are sourced from the Chinese Resource and Environmental Science and Data Center.

2.3. Assessment of Vegetation Ecological Sensitivity in the Research Experimental Area

Centering around the Xining and Jianghe station sites on the Qinghai–Tibet Railway, experimental buffer zones are established with radii of 5 km, 10 km, 15 km, 30 km, and 40 km along both sides of the railway line. In each area, 500 random points are selected, ensuring an equal representation of each land cover type. The mean NDVI (Normalized Difference Vegetation Index) values over several years are calculated using Landsat data. The boxplot distribution patterns within the 5 km, 10 km, 15 km, 30 km, and 40 km spatial regions based on the NDVI mean values are illustrated in Figure 2.

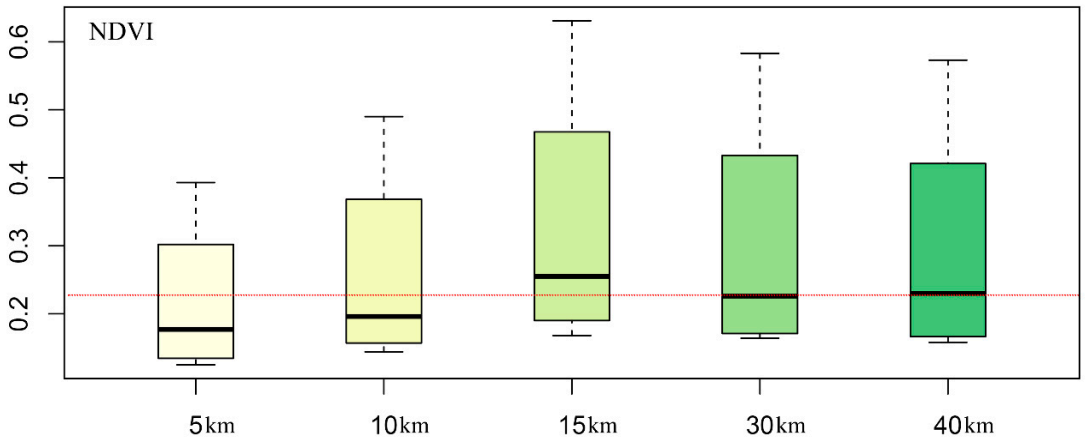

Figure 2. Mean NDVI Spatial Boxplot Statistical Distribution Diagram.

From Figure 2, it can be observed that the multi-year average NDVI values exhibit distinct characteristic distributions within the 5 km, 10 km, 15 km, and 30 km spatial areas, while showing essentially the same stability characteristics within the 30 km and 40 km regions. Based on this observation, the buffer radius along both sides of the railway in the research area is 30 km.

2.4. Synthesis and Evaluation of RSEI Based on GEE

2.4.1. Other Data and Preprocessing

To select data for the target year and the summer months (June to September) of the preceding and following year, images with cloud cover of less than 15% are filtered on the GEE (Google Earth Engine) cloud platform. The QA quality band is used for cloud masking to create a composite image with minimal cloud content. To avoid interference from water bodies, an improved Normalized Difference Water Index (MNDWI) is used to extract a water body threshold, and water bodies are masked accordingly. In this study, vegetation indices, moisture components, soil indices, and surface temperature are used to represent greenness, wetness, dryness, and heat indicators, respectively. Based on these, an RSEI model is constructed (Formula (1)).

$$\mathrm{RSEI} = \mathrm{f}(\ \mathit{Greeness}\ ,\ \mathit{Heat}\ ,\ \ \mathit{Wetness}\ ,\ \mathit{Dryness}\ ) \tag{1}$$

In Formula (1), Greenness is the greenness index, represented in this paper by the NDVI index derived from Landsat data. Heat represents the heat component and is characterized in this paper by daytime LST (Land Surface Temperature) products retrieved from Landsat series data. Wetness is the wetness component, and Dryness is the dryness component. The wetness component is obtained as the third component (Wet) from the tasseled cap transformation of Landsat multispectral imagery from different sensors. The dryness component is represented by the Normalized Difference Built-up and Soil Index (NDBSI) as proposed by Xu and Hu [38]. After calculating the four components that characterize the quality of the ecological environment based on Landsat data, these components are dimensionlessly normalized. Subsequently, the principal component analysis (PCA) method is employed. This approach is used in the multi-index synthesis process to avoid biases arising from factors such as arbitrarily determined weights and correlations between the indices. The main information derived from the multi-index synthesis in the experimental area is predominantly distributed in the first principal component. Therefore, in this study, the first component obtained after principal component analysis (PCA) of the multi-component indices is normalized to represent the RSEI, which indicates the quality of the environmental ecology.

2.4.2. Assessment of the Suitability of RSEI

To verify the applicability of the RSEI along the Qinghai–Tibet Railway, this paper selects the area surrounding the Xining railway station as the experimental area for the method. The principal component eigenvalues, eigenvectors, and the contribution rates of each principal component are calculated, with the parameters presented in Table 1.

Table 1. Eigenvalues, eigenvectors, and contribution rates of principal components.

Time (Year)		PCA			
		1	2	3	4
2020	NDVI	0.581622	−0.445190	0.401402	0.549911
	LST	−0.395860	−0.779870	−0.467510	0.128590
	Wet	0.461116	0.285071	−0.780050	0.312462
	NDBSI	−0.540720	0.335183	0.108816	0.763826
	Eigenvalue	0.272998	0.031129	0.013628	0.004649
	Contribution rate %	84.6	9.7	4.2	1.4

Table 1 indicates the following:

(1) The paper calculates the PCA starting with the NDVI as the initial indicator. From the loading matrix, it can be observed that the indices representing greenness and wetness, namely, NDVI and Wet, have a positive influence on the RSEI. Conversely, the indices representing heat and dryness, LST (Land Surface Temperature) and NDBSI (Normalized Difference Built-up and Soil Index), show negative values. This is consistent with many studies on soil moisture effects, where greenness and wetness are shown to have a positive impact on the environment, whereas temperature and dryness tend to have a negative impact on the ecological environment [44].

(2) Among the four components of the principal component analysis, it is found that the first component accounts for approximately 85% of the characteristics of each indicator. Therefore, it can be used to represent other components to comprehensively characterize the quality of the ecological environment.

In summary, the RSEI is well-suited for application along the Qinghai–Tibet Railway. The above processes in this study are all calculated and implemented based on the Google Earth Engine platform. The masking of water bodies helps avoid interference from large water areas in the region on the surface wetness factor.

2.5. Optimal Parameters-Based Geographical Detector (OPGD) Model

The geodetector is a set of statistical methods used to detect spatial differentiation and reveal its driving forces. By calculating and comparing the single-factor q-values and the q-values after the overlay of two factors, it analyzes the interactions between variables [35]. This method has been widely applied in geoscience research. In this study, the OPGD model [45] is selected. This model optimizes the empirical decision-making regarding the discretization of spatial data and the spatial scale effect issues commonly found in standard geographical detector models. The study uses regional elevation and land use type as spatial stratification variables, with the Remote Sensing Ecological Index (RSEI) as the dependent variable. Mean temperature (tmp), mean precipitation (pre), and Human Activity Intensity Index (HAII) are used as explanatory variables. The study employs a 1 km spatial grid scale to explore the different spatial driving contributions of each driving variable to RSEI.

2.5.1. Factor Detection

As the core part of the geodetector, the factor detector reveals the relative importance of explanatory variables through the Q statistic. The Q statistic is used to compare the

variance of observations across the entire study area with the variance within layers of the variable. The formula for calculating the Q value is as follows:

$$Q_v = 1 - \frac{\sum_{j=1}^{M} N_{v,j}\sigma_{v,j}^2}{N_v\sigma_v^2} \quad (2)$$

In the formula, N_v and σ_v^2 represent the total number of observations and the overall variance in the entire study area, respectively. $N_{v,j}$ and $\sigma_{v,j}^2$ represent the number of observations and the overall variance within the (j = 1. . .M) subregion for the variable. A higher Q value indicates greater importance of the variable. This is because it implies a smaller variance within subregions and a larger variance between subregions. The Q value measures the degree to which a factor explains the quality of the ecological environment, with a range from 0 to 1. The closer the Q value is to 1, the stronger the explanatory power of the factor on the quality of the ecological environment, meaning a greater impact, and vice versa.

2.5.2. Risk Detection

Risk detectors are used to test whether there are significant differences between subregions classified or stratified by certain categories or variables, as represented by spatial patterns of mean values. The t-test is used to test the difference between the mean values of subregions a and b.

$$t_{Y_\eta - \overline{Y}_\kappa} = \left(\overline{Y}_\eta - \overline{Y}_\kappa\right) / \sqrt{\frac{s^2{}_\eta}{N_\eta} - \frac{s^2{}_\kappa}{N_\kappa}} \quad (3)$$

$\overline{Y}_\eta$ and $\overline{Y}_\kappa$ are the mean values of observations in subregions η and κ, respectively. $s^2{}_\eta$ and $s^2{}_\kappa$ are the sample variances, and N_η and N_κ are the numbers of observations in each subregion, respectively. The degrees of freedom for this statistic, which is approximately distributed as a t-distribution, are as follows:

$$df = \left(\frac{s^2{}_\eta}{N_\eta} + \frac{s^2{}_\kappa}{N_\kappa}\right) / \left[\frac{1}{N_\eta - 1}\left(\frac{s^2{}_\eta}{N_\eta}\right)^2 + \frac{1}{N_\kappa - 1}\left(\frac{s^2{}_\kappa}{N_\kappa}\right)^2\right] \quad (4)$$

Therefore, under a given significance level, the null hypothesis: $H_{0:}\ \overline{Y}_\eta = \overline{Y}_\kappa$ can be tested using the t-distribution. In this paper, the significance level is set at 0.05.

2.5.3. Interactive Detection

The interactive detector uses the Q value from the factor detector to calculate the relative importance of interactions, determining the interactive effects of two overlapping spatial variables. Spatial interaction is the overlay of two spatial explanatory variables. The interactive detector explores the nature of the interaction by comparing the Q value of the interaction with those of the two individual variables. This interaction explains whether the impact of the two spatial variables is weakened, enhanced, or independent of each other. The interactive detector explores five types of interactions, including nonlinear weakening, single-variable weakening, bivariate enhancement, independence, and nonlinear enhancement (Table 2) [46]. Therefore, the results of the interaction detector include both the Q value of the interaction and the type of interaction.

Table 2. The interaction between two explanatory variables and the impact of their interaction.

Geographic Interactions	Interactions
$Q_{u\cap v} < min(Q_u, Q_v)$	Nonlinear weakening: The influence of a single variable is nonlinearly weakened by the interaction of two variables.
$min(Q_u, Q_v) \le Q_{u\cap v} \le max(Q_u, Q_v)$	Single-variable weakening: The impact of a single variable is weakened due to the interaction, resulting in a reduced effect of that single variable.
$max(Q_u, Q_v) < Q_{u\cap v} < (Q_u + Q_v)$	Bivariate enhancement: The impact of a single variable is enhanced through interaction, leading to a bivariate enhancement.
$Q_{u\cap v} = (Q_u + Q_v)$	Independence: The impact of the variables is independent.
$Q_{u\cap v} > (Q_u + Q_v)$	Nonlinear enhancement: The impact of the variables shows a nonlinear enhancement.

2.5.4. Ecological Detection

The ecological detector is used to test whether one explanatory variable has a higher impact compared to another explanatory variable. The F statistic is used to test the significance of the different impacts of explanatory variables.

$$F = \frac{N_\mu (N_\nu - 1)\sum_{j=1}^{M_\mu} N_{\mu,j}\sigma_{\mu,j}^2}{N_v (N_\mu - 1)\sum_{j=1}^{M_v} N_{v,j}\sigma_{v,j}^2} \tag{5}$$

2.6. Pixel-Based Method for Calculating Ecological Environment Quality Matrix Transition

The theory of land use transition matrices originates from the quantitative characterization of states and state transitions in system analysis. It can be used to reflect the process of mutual transformation between different land cover types from the beginning to the end of a specific period. The general formula for land use transition matrices is as follows:

$$S_{ij} = \begin{pmatrix} S_{11} & \cdots & S_{1n} \\ \vdots & \ddots & \vdots \\ S_{n1} & \cdots & S_{nn} \end{pmatrix} \tag{6}$$

Drawing on this theory, we define a per-pixel ecological quality matrix method to calculate the spatial transition states of ecological quality over different periods. Therefore, in Formula (6), S represents the area of each pixel, and n represents the ecological quality levels before and after the transition; i and j indicate the transition of ecological quality level i before the transition to level j after the transition in terms of pixels. In the matrix, each row element represents the source information of the pixels of ecological quality level j after the transition, derived from the ecological quality level i before the transition.

3. Results

3.1. Analysis of the Spatiotemporal Variation in Ecological Environmental Quality along the Qinghai–Tibet Railway

The overall performance of the ecological environment quality along the Qinghai–Tibet Railway from Xining to Jianghe station is shown in Figure 3. The research uses the significant time nodes of railway construction between 1986 and 2020 as temporal segmentation points. The analysis of the spatiotemporal statistical distribution of the RSEI from 1986 to 2020 along the Xining–Jianghe Railway region shows that over 30 years, the overall regional ecological quality has been stable and improving. However, within this period, during the phase of the first railway project completion between 1986 and 1994, the

average RSEI was less than 0.40 and slightly declined. This indicates a slight decrease in the overall ecological quality of the region in the first 10 years after the railway opened. After 2002, the overall ecological quality began to recover, with the RSEI average exceeding 0.50. During the second phase of railway construction from 2002 to 2007, there was a slight downward trend in RSEI values. After 2007, the RSEI average began to stabilize and increase, reaching 0.53 by 2020. Over the 20 years from 2001 to 2020, the overall ecological quality of the region showed signs of improvement. Throughout the various stages of railway construction, RSEI values were mainly distributed between 0.20 and 0.80, with the relative change in ecological quality each year being less than 0.30. Around 1994, the overall distribution of RSEI values was at its lowest, while in 2020, it was at its highest.

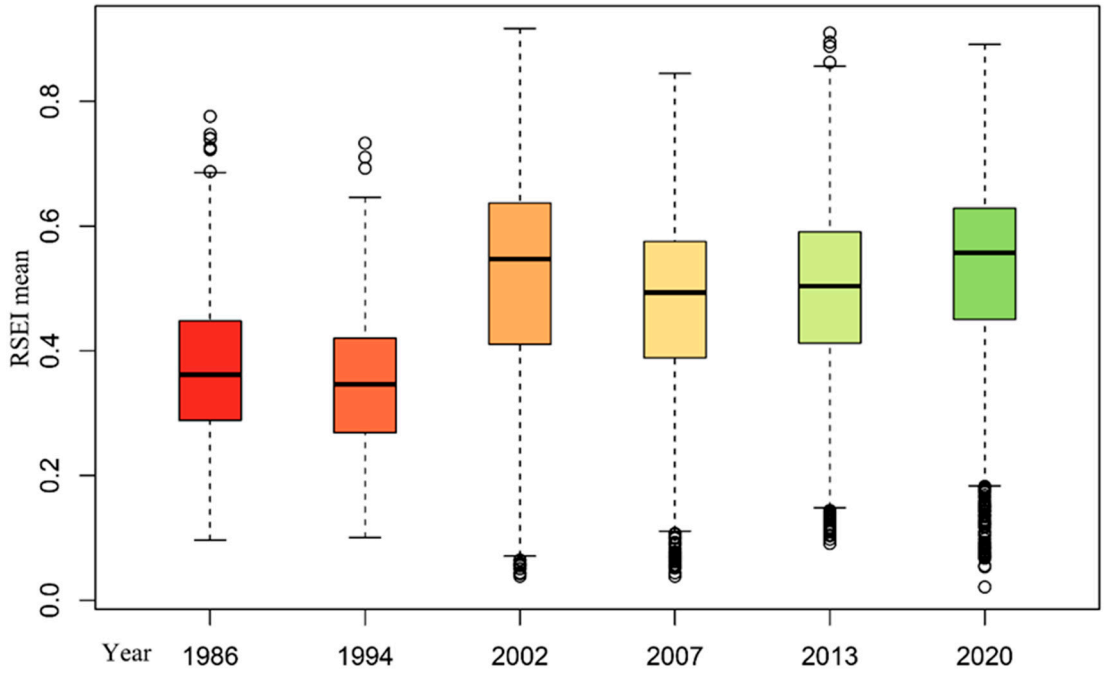

Figure 3. Statistical distribution map of the mean RSEI values along the Qinghai–Tibet Railway.

Based on the distribution of RSEI values, this study classifies the ecological quality of the region into the following quantitative grades: I (0.2–1.0) (worst), II (0.2–0.4) (poorer), III (0.4–0.6) (moderate), IV (0.6–0.8) (good), and V (0.8–1.0) (best). In this classification, Level I represents the worst quality grade, while Level V represents the best quality grade. From the area proportion of each ecological grade within this section (as shown in Figure 4), it can be observed that:

(1) Throughout the years, the areas classified as Level II and Level III have the highest proportions. The area proportion of the Level III regions is relatively stable, with the percentages in different years being 35.80% in 1986, 30.27% in 1994, 42.30% in 2002, 55.30% in 2007, 55.60% in 2013, and 46.60% in 2020. The area proportion of Level II regions shows a slightly larger fluctuation range. The percentages in different years are 58.90% in 1986, 63.00% in 1994, 18.60% in 2002, 23.80% in 2007, 18.70% in 2013, and 13.40% in 2020. The area proportions of the worst and best ecological quality levels (presumably Levels I and V) are similar, both being around 10.00%.

(2) The ecological quality of the Xining–Jianghe section is primarily moderate and good. Notably, there was a significant increase in the proportion of areas classified as Level III and IV in 2002. Despite this increase, the area proportions of these levels have consistently exceeded 50.00% in each year, indicating that the overall ecological quality of this region is in a state of continuous recovery.

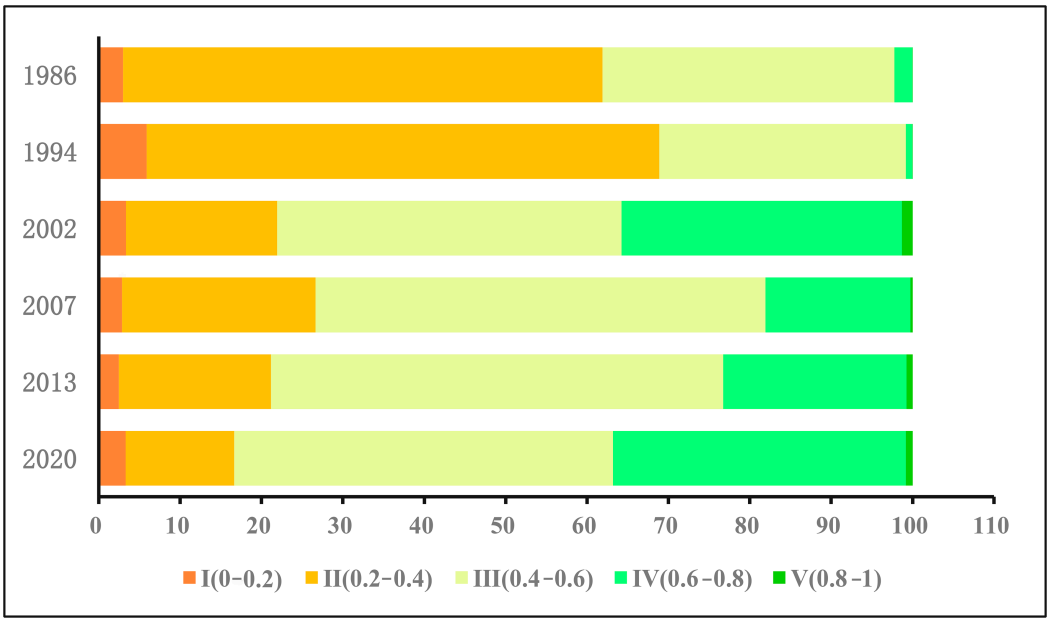

Figure 4. Statistical Chart of Proportion of Area by Different Ecological Quality Levels.

Quality Levels From the spatiotemporal distribution maps of ecological quality in the region along the Qinghai–Tibet Railway from Xining station to Jianghe station (Figures 5 and 6), it can be observed that there is a clear spatial heterogeneity in the distribution of RSEI (Remote Sensing Ecological Index) values within this section. Firstly, the RSEI characteristic values in the areas near the railway line are mostly between 0 and 0.4, indicating that the ecological quality is at a poorer level. Furthermore, it is observed that the ecological quality in the urban areas around the Xining station, the surrounding mountainous regions, the bare soil areas near Qinghai Lake, and the areas around the Jianghe station influenced by the railway and highway is significantly lower than in other areas, especially lower than the less trafficked areas on the right side of the railway line from Xining to Jianghe. From the perspective of spatiotemporal distribution, during the period from 1986 to 1994, the overall ecological quality along the Qinghai–Tibet Railway was relatively poor, with the majority of the RSEI spatial distribution values being less than 0.4. In 2002, the ecological quality within the region began to recover, and between 2007–2020, the region stabilized. It mainly showed that the ecological quality in urban areas along the railway stations was relatively poorer, with the majority of the RSEI spatial distribution falling within the categories of Level I (0.2–1.0), II (0.2–0.4), and III (0.4–0.6). Other areas tended towards stable recovery, with their RSEI spatial distribution predominantly in the Level IV (0.6–0.8) and V (0.8–1.0) categories.

It can be observed that by 2020, most areas within a 30 km radius along the Qinghai–Tibet Railway will be in a stable state with good ecological quality. However, the areas radiating from each railway station exhibit distinctly poorer ecological quality. This is most notable around the Xining station's urban area and the lakeside area near the Qinghai Lake station (Figure 7). Additionally, the areas surrounding Huangyuan station, Gangcha station, and Jianghe station also exhibit relatively poorer ecological quality.

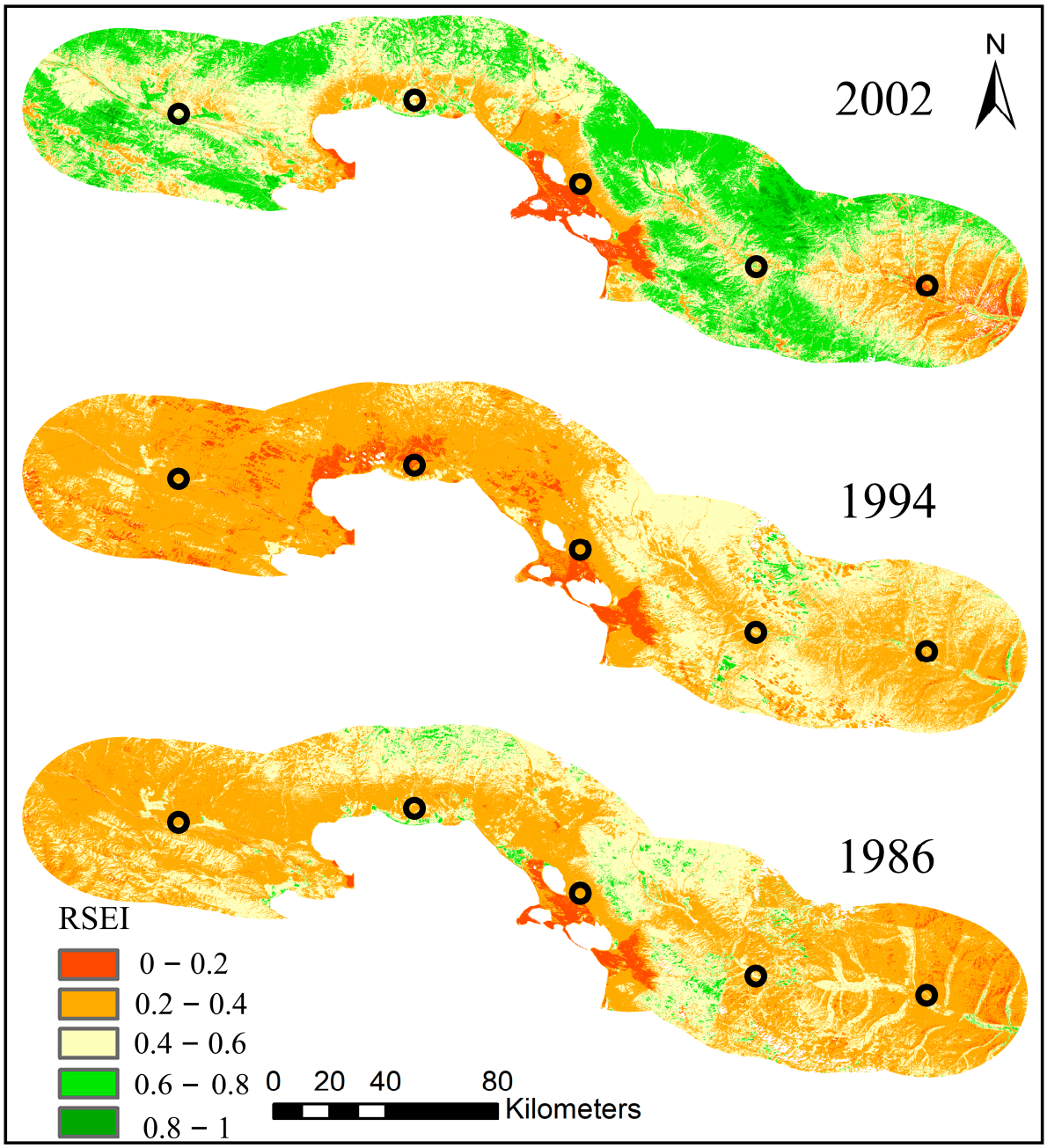

Figure 5. Spatiotemporal distribution map of ecological quality in the area along the Qinghai–Tibet Railway, 1986–2002.

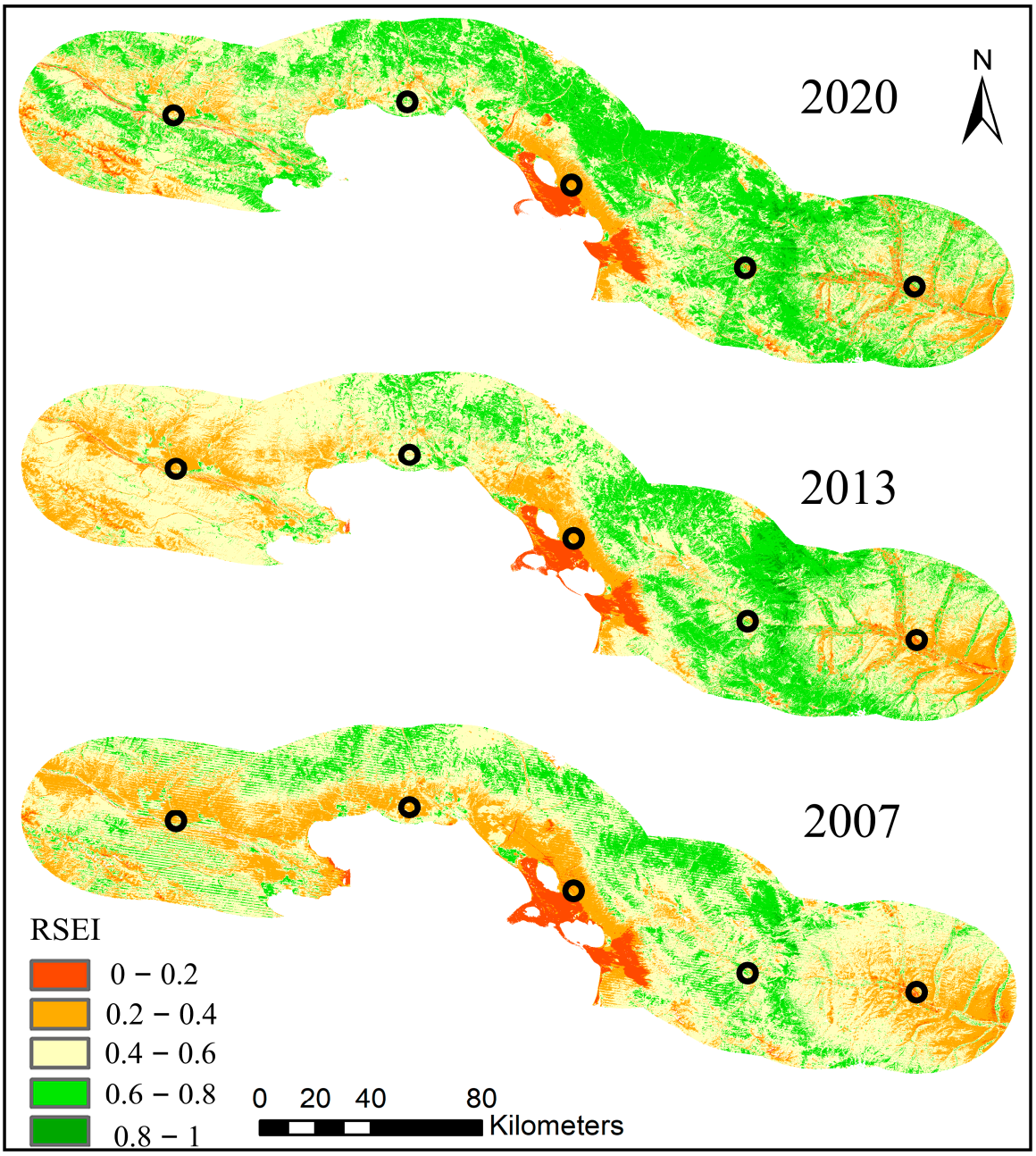

Figure 6. Spatiotemporal distribution map of ecological quality in the area along the Qinghai–Tibet Railway, 2007–2020.

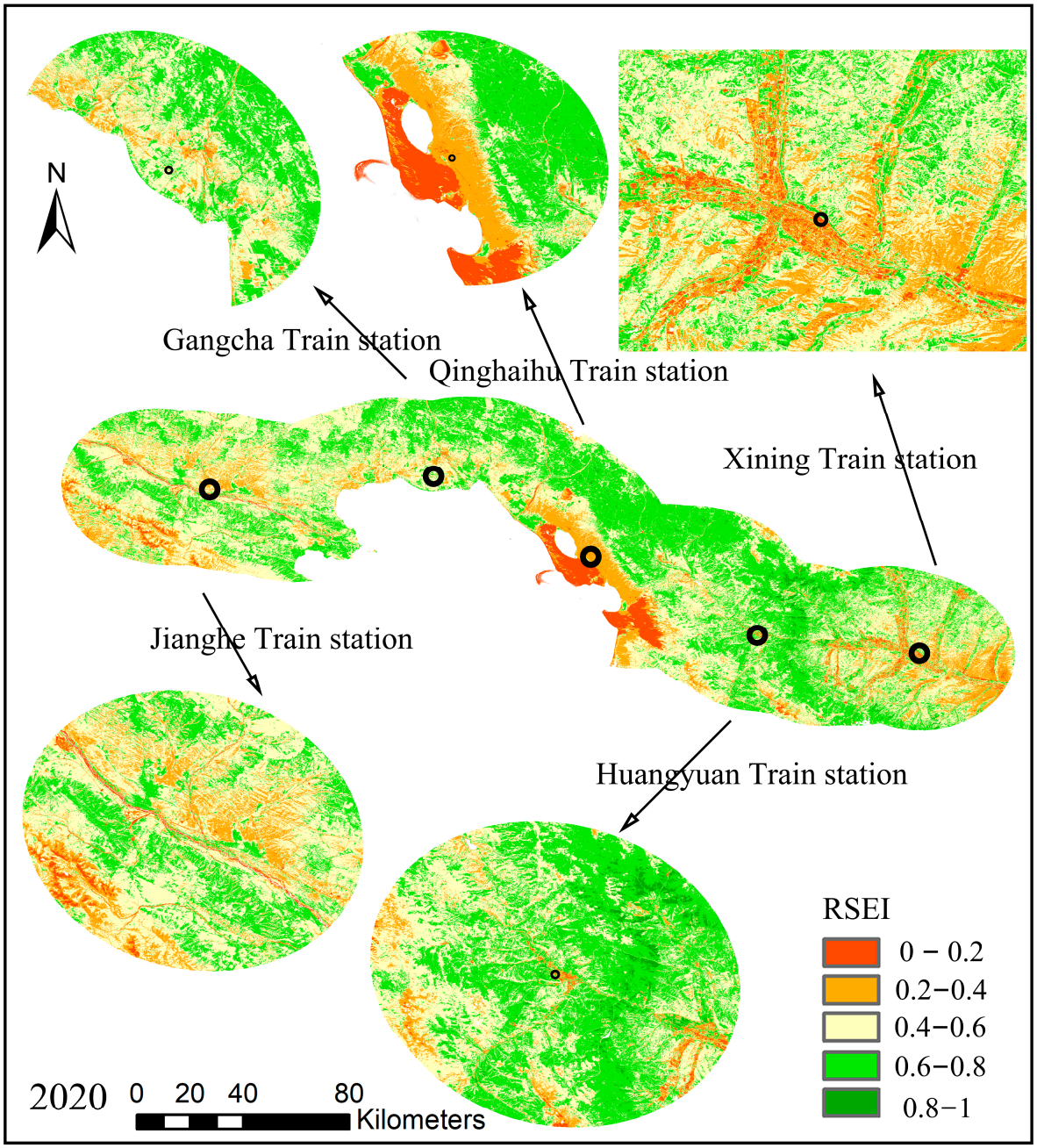

Figure 7. Spatiotemporal distribution map of ecological quality in the area along the Qinghai–Tibet Railway, 1986–2020.

Taking a 30 km radius around the train stations along the Qinghai–Tibet Railway from Xining to Jianghe as the focus, a statistical analysis within the buffer zones of each station (Figure 8) reveals that the average RSEI values around the Xining station, which is primarily influenced by the city and tourism, and around Qinghai Lake are consistently less than 0.6 in various years, categorizing these stations as having poorer ecological quality. However, since the railway's operation began in 1986, the overall ecological quality has shown a trend of improvement. In the areas around the Huangyuan, Jianghe, and Gangcha railway stations, where human activities are relatively limited, the average RSEI values are comparatively higher. Since 2002, these values have generally tended towards 0.6, indicating these areas as having better ecological quality recovery. However, the overall average RSEI values within the 30 km radius of each railway station are still less than

0.6, suggesting that the construction and operation of the railway have had a significant impact on the changes in the surrounding ecological environmental quality. From the analysis of the RSEI average heat map features, it can be observed that along the Qinghai–Tibet Railway from Xining to Jianghe stations, the Xining station exhibits strong spatial characteristics. In the years 1990, 2002, and 2007, it shows strong temporal characteristics, which align with the timeline of various construction and operational phases of the railway.

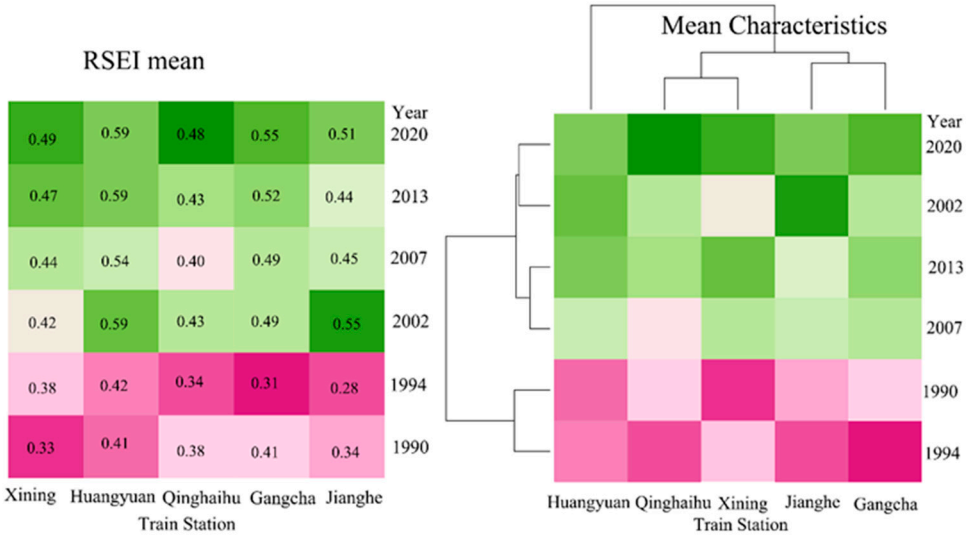

Figure 8. Statistical Analysis of Buffer Zone Data for Train Stations along the Qinghai–Tibet Railway.

3.2. Analysis of the Dynamic Changes in Ecological Environmental Quality during Various Railway Construction Phases

Combining the definitions of each ecological level in Section 3.1, this study defines the rules of change for different types of ecological quality after matrix transition. The difference in ecological quality levels between the previous year and the following year, with a value range of −4 to −3 (1–5, 1–4, 2–5), is categorized as a significant improvement, −2 to −1 as a mild improvement, 0 as unchanged, 1 to 2 as a mild deterioration, and 3 to 4 as a significant deterioration. The specific corresponding relationships are shown in Table 3.

Table 3. Types of ecological environmental quality grade transition matrices along the railway.

Correspondence of Ecological Level Changes	5 (V)	4 (IV)	3 (III)	2 (II)	1 (I)
5 (best)	5-5 (no change)	5-4 (mild deterioration)	5-3 (mild deterioration)	5-2 (significant deterioration)	5-1 (significant deterioration)
4 (good)	4-5 (slight improvement)	4-4 (no change)	4-3 (mild deterioration)	4-2 (mild deterioration)	4-1 (significant deterioration)
3 (moderate)	3-5 (slight improvement)	3-4 (slight improvement)	3-3 (no change)	3-2 (mild deterioration)	3-1 (mild deterioration)
2 (poorer)	2-5 (significant improvement)	2-4 (slight improvement)	2-3 (slight improvement)	2-2 (no change)	2-1 (mild deterioration)
1 (worst)	1-5 (significant improvement)	1-4 (significant improvement)	1-3 (slight improvement)	1-2 (slight improvement)	1-1 (no change)

Based on the ecological quality matrix transition, the statistical and spatial distribution results of changes among different ecological quality types during various construction

stages along the Qinghai–Tibet Railway are as shown in Figure 9. It can be observed that (1) during the first 10 years of railway operation, from 1986 to 1994, the ecological quality recovery was slow, predominantly characterized by no change. From 1994 to 2002, most areas began to show mild improvement in ecological quality, with the overall ecological recovery areas accounting for nearly 70%. Between 2002 and 2007, the period of the second phase extension of the railway line, the predominant change was again no change, accounting for about 60%. However, during this period, about 30% of the area experienced a mild deterioration in ecological quality. From 2007 to 2020, the ecological quality changes along the railway tended to stabilize. The areas with no change in ecological quality accounted for over 50%. Among the areas that did experience change, the majority, about 25%, showed mild improvement, while around 10% experienced mild deterioration. (2) During the different construction phases of the Qinghai–Tibet Railway, the ecological quality levels primarily exhibited no change or mild changes. Over the span of more than 30 years from 1986 to 2020, the overall trend was a mild improvement in ecological quality. Thus, it can be concluded that throughout the various construction periods along the Qinghai–Tibet Railway, the overall change in ecological quality has been predominantly stable and inclined towards improvement. (3) In the types of ecological quality changes that occurred, the majority were characterized by mild improvement and mild deterioration, with the proportion of mild improvement being generally larger than that of mild deterioration. The types of significant improvement and significant deterioration were the least common, accounting for less than 1% in all segments. Therefore, when considering the entire Qinghai–Tibet Railway, the overall change in ecological quality levels was predominantly characterized by mild improvement. This trend was particularly prominent during the 1994–2002 period, significantly more than in the other four time segments considered in this study.

From 1986 to 2020, in the spatiotemporal distribution change map of the ecological environmental quality along the Xining to Golmud section of the Qinghai–Tibet Railway (Figure 9), it is observed that over the entire period from 1986 to 2020, the regions experiencing changes in ecological quality exhibit a certain degree of spatial heterogeneity. Along the railway, particularly in the urban areas surrounding the Xining and Qinghai Lake stations, a mild deterioration in ecological quality is evident. Furthermore, within these mildly deteriorating areas, there are smaller regions where significant deterioration in ecological quality is observed. In contrast, other areas mainly show mild improvements in ecological quality. Notably, regions showing significant improvements in ecological quality are primarily located within a 15–20 km radius around Xining to Huangyuan.

Further combining the analysis of the specific type changes in ecological quality flow from 1986 to 2020 (Figure 10), it can be concluded that over the past 30 years, the main ecological quality change has been a mild improvement from poorer to medium types (II–III), with this change covering 31.75% of the area. The next slight change is a mild improvement from medium ecological quality to good quality (III–IV), accounting for 19.91% of the area, followed by a mild improvement from poorer ecological quality to better quality, which covers 14.48% of the area (II–IV). Other types of mild improvements in ecological quality include changes from the poorest ecological quality to poorer quality (I–II), from good ecological quality to the best quality (IV–V), from the poorest to medium quality (I–III), and from medium quality to the best quality (III–V). The area percentage of these types of ecological quality changes is less than 1.00%. Significant improvements and significant deteriorations in ecological quality also occurred, but their combined area percentage is less than 0.50%. Moreover, the area percentage for the mildly worsening type of ecological quality is 3.57%. The primary direction of this change is from medium ecological quality to poorer quality (III–II), which accounts for 1.40% of the area, and from poorer ecological quality to the poorest quality (II–I), which accounts for 1.34% of the area. The area percentage for the other types of change is less than 1.00%. Among the types with no changes, the medium ecological quality and the poorer ecological quality types have the largest area percentages, accounting for 13.83% and 11.09%, respectively.

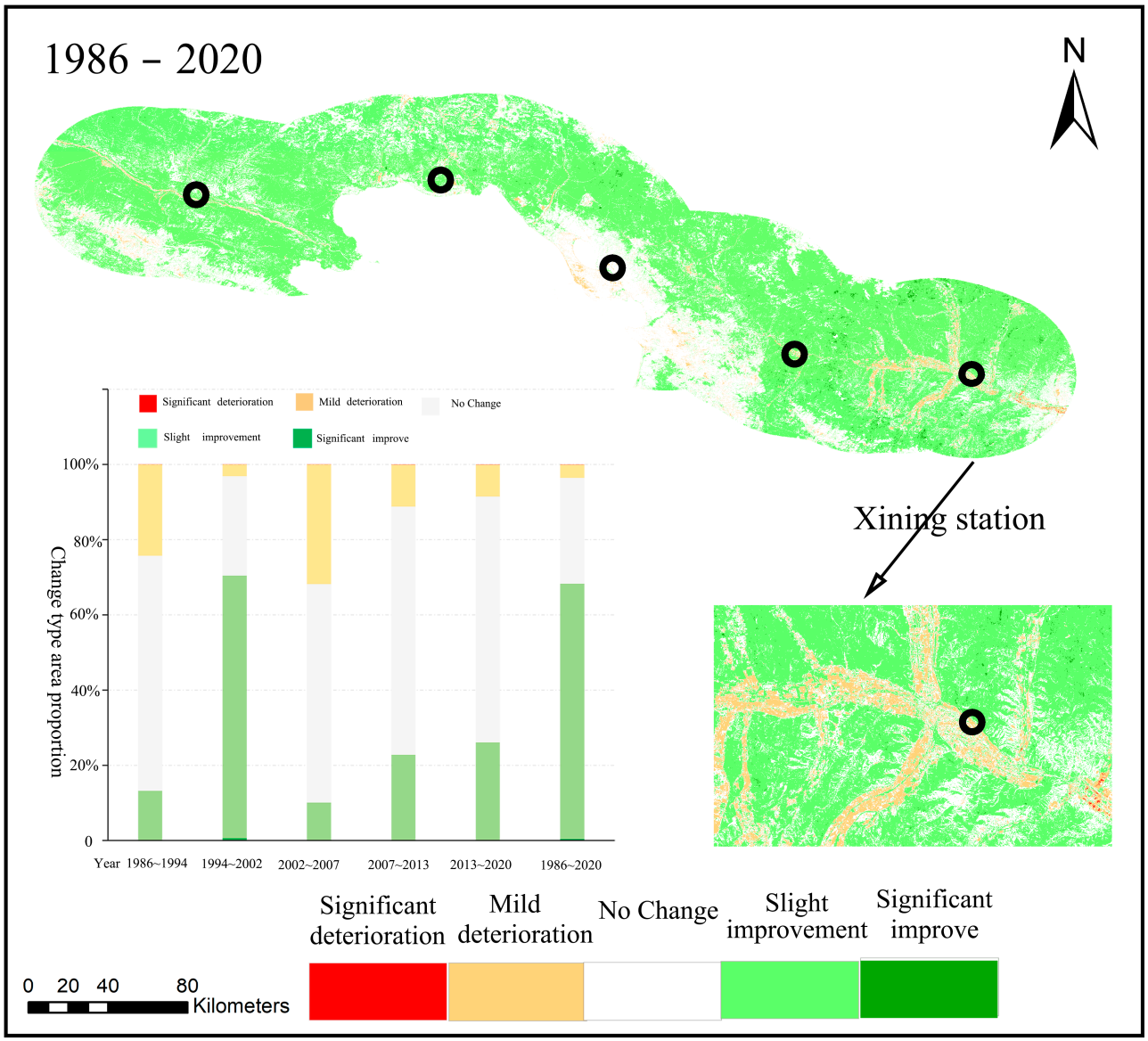

Figure 9. 1986–2020 distribution map of ecological quality type changes.

3.3. Analysis of the Driving Factors for Spatiotemporal Changes in Ecological Environmental Quality along the Qinghai–Tibet Railway

3.3.1. Optimal Parameter Discretization Results for Continuous Explanatory Variables

In this study, the explanatory variables used are the Human Activity Intensity Index (HAII) calculated per pixel along the railway area, the annual average temperature (Atmp), and the annual average precipitation (Apre), all of which are continuous variables. Therefore, it is necessary to first discretize them spatially. The parameter optimization selection process and results for the OPGD model are shown in Figure 11.

The results indicate that for different explanatory variables within the area along the Xining–Golmud section of the Qinghai–Tibet Railway, the optimal combination of discretization methods and the number of breakpoints varies. The optimal parameter combinations for the precipitation factor, temperature factor, and human activity intensity factor are quantile breakpoints with 7, 5, and 6 intervals, respectively (Figure 11a). Furthermore, by combining the different numbers of breakpoints and evaluating the optimization methods for each parameter based on the Q values, it is found that the optimal discretization method for the precipitation factor and human activity intensity factor is the quantile method, whereas, for the temperature factor, the equal interval method is optimal.

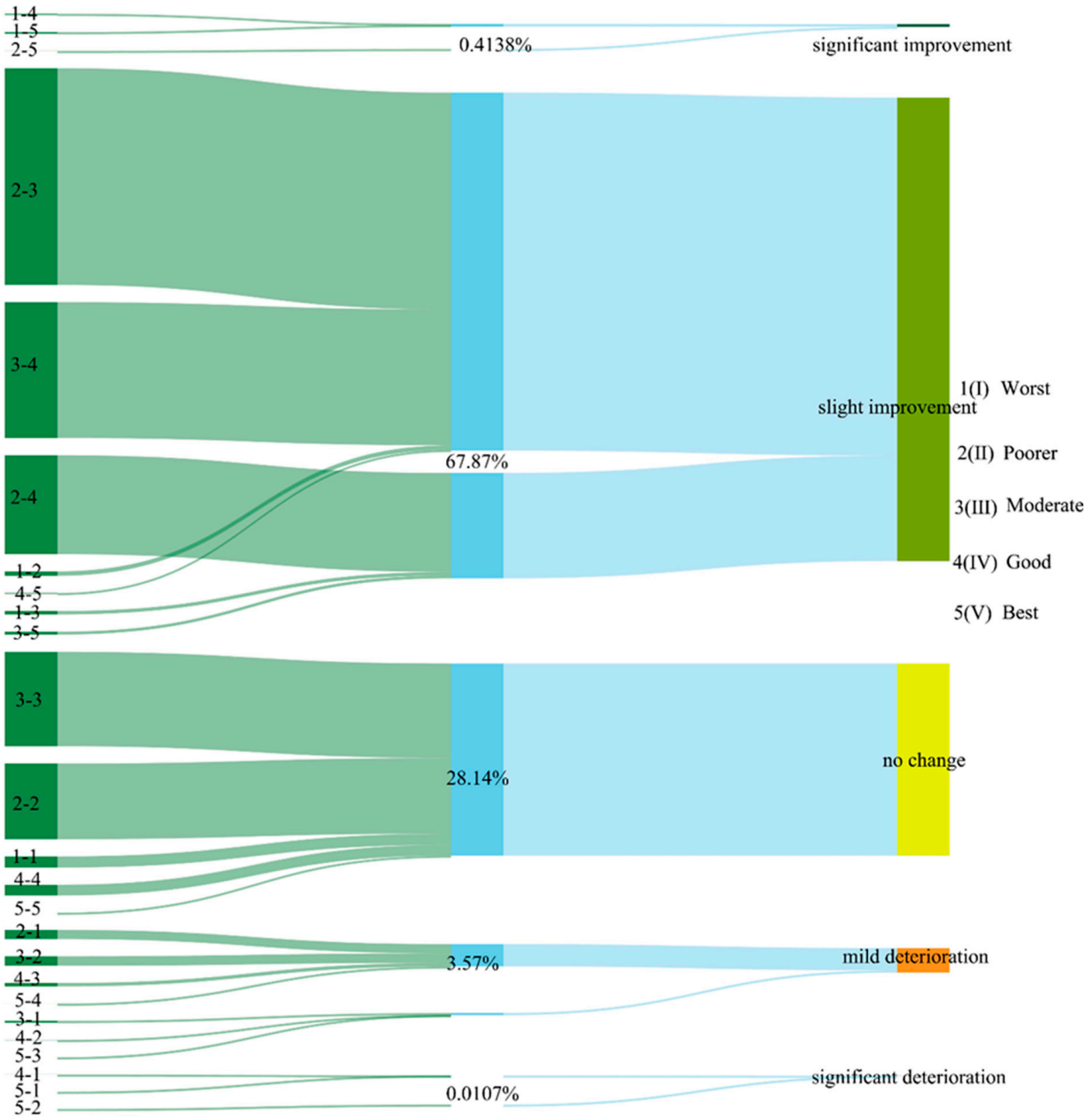

Figure 10. 1986–2020 statistical distribution map of ecological quality level flow changes along the Qinghai–Tibet Railway.

3.3.2. Optimal Parameter Discretization Results for Continuous Explanatory Variables

After spatially discretizing each explanatory variable, they are utilized in a geographic detection model. Based on the factor detector model, the impact of individual factors such as elevation, land use type, temperature, precipitation, and human activity intensity on the spatial variability of ecological quality is calculated. The results of these calculations are shown in Figure 12. It can be observed that for the area along the Xining–Golmud section of the Qinghai–Tibet Railway as a whole, each explanatory variable significantly drives the spatial changes in ecological quality, with all *p*-values being 0. The ranking of the impact of each factor is as follows: land use type > human activity intensity > temperature > precipitation > altitude. Their corresponding Q values are 0.1530, 0.1354, 0.1353, 0.1181, and

0.0697, respectively. Land use type is the key factor in the spatial variability of ecological quality along the Xining–Golmud section, with human activity intensity, temperature, and precipitation also having a high impact, while the influence of altitude differences is relatively smaller.

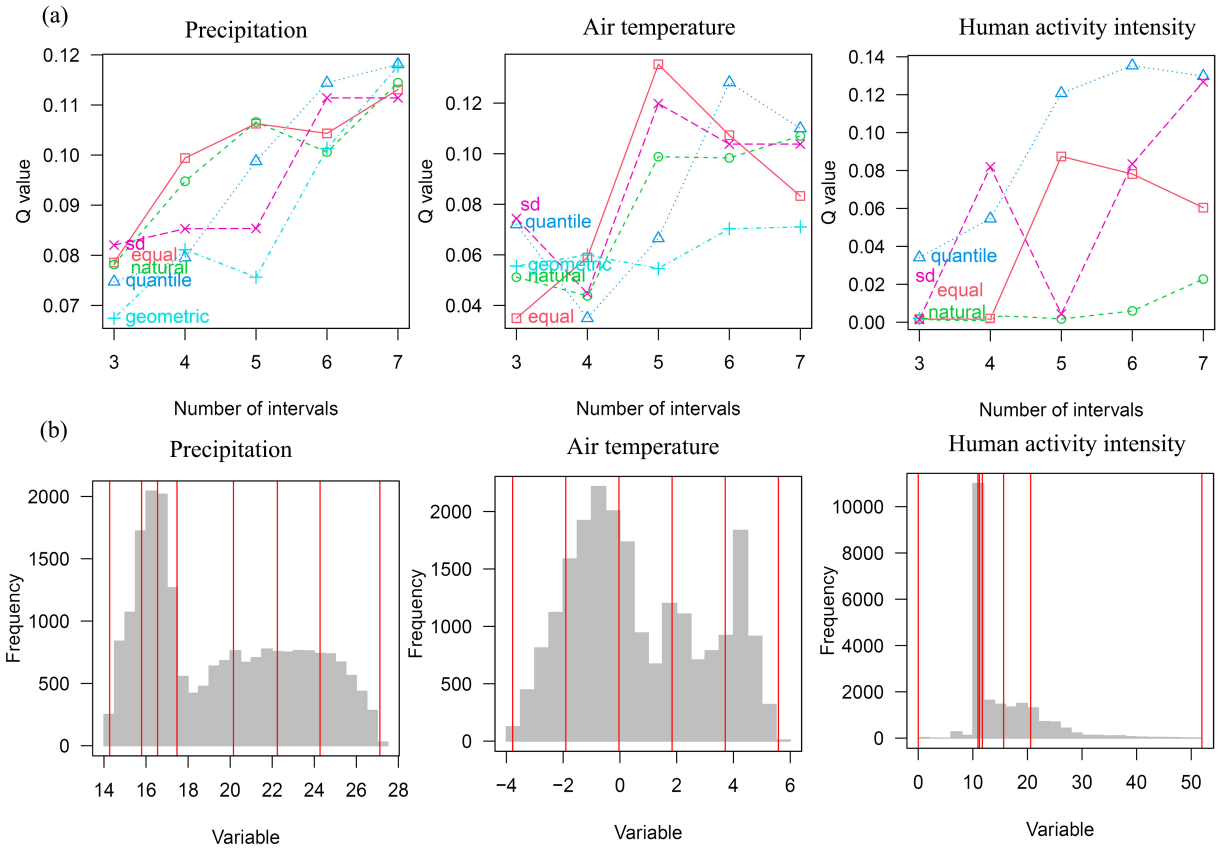

Figure 11. (**a**,**b**) Optimal discretization process for continuous variable parameters in the geodetector model.

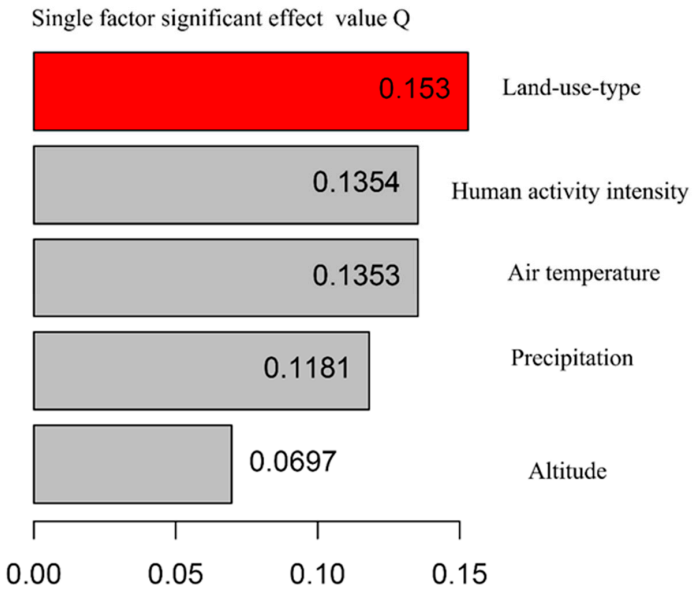

Figure 12. Driving values of various factor variables on the spatiotemporal changes in ecological quality along the Qinghai–Tibet Railway.

3.3.3. Analysis of Risk Detection for Ecological Quality Changes Due to Spatial Partitioning of Various Factors

This approach involves further utilizing the spatial stratification of each explanatory variable and applying a risk detector model to quantitatively analyze the impact of these variables on spatial variations in ecological quality within different spatial regions. This method allows for the identification of the variation in risk levels for ecological quality changes across different spatial areas. From Figure 13, it is evident that within the Xining to Jianghe section, there are significant differences in the impact of various driving variables on ecological quality change, based on their different spatial distributions. For each driving factor, there are three impact zones: high, medium, and low. Notably, elevation within the 2500–3000 m range poses the highest risk to ecological quality change, with an average risk value of 0.20. For land use, areas categorized as agricultural land have the strongest risk of driving ecological quality change, with an average risk value of 0.15. In terms of annual average precipitation, the range of 22 to 24 mm has the highest impact on ecological quality change, with a risk value of 0.35. Regarding average annual temperature, the range of 1.84 to 3.71 degree centigrade is the most influential in driving ecological quality change, with an average risk value of 0.40. For human activity intensity, regions with characteristic values between 10.90 and 11.20 have the strongest impact on ecological quality change, with an average risk value of 0.25.

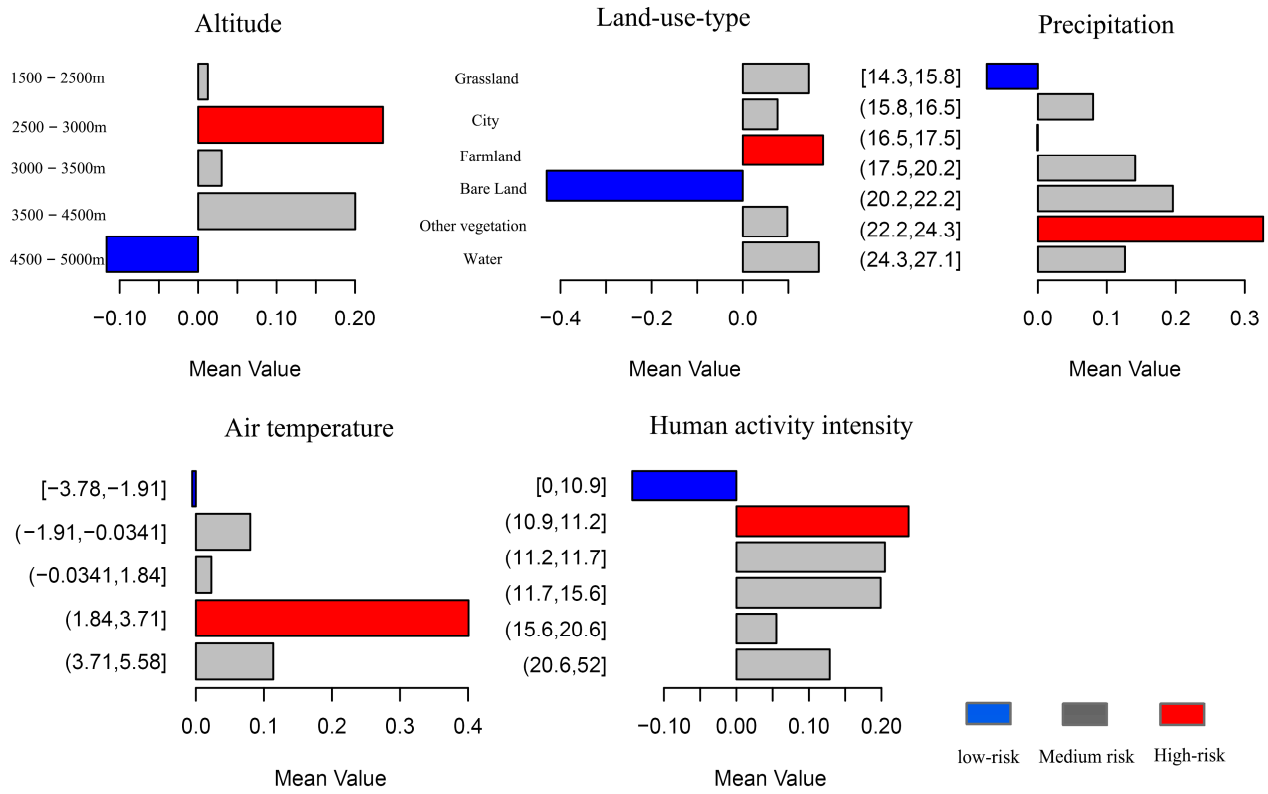

Figure 13. Risk values of various driving factors on ecological quality changes in spatial stratification.

To further quantify the risk areas for ecological quality changes among various factors, the spatial distribution of the risk of ecological quality change along the Xining–Jianghe section of the Qinghai–Tibet Railway was determined by each explanatory variable. The results of this spatial distribution of ecological quality change risk are shown in Figure 14. It is observed that the risk distribution areas of various explanatory variables exhibit a certain degree of spatial similarity. The impact on ecological quality change around the Xining station is relatively high overall. Then, moving along the direction from Xining to

Jianghe, the impact gradually decreases, with the driving influence being relatively the smallest around the Jianghe station area.

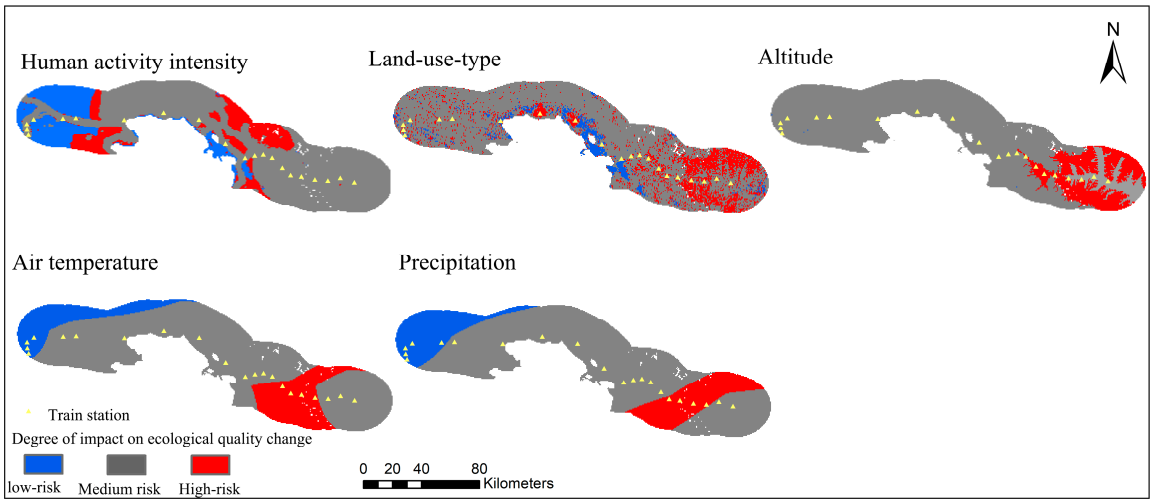

Figure 14. Distribution of risk detection for ecological quality changes due to various driving factors in spatial stratification.

This study, using a significance level test of 0.05, further assesses whether the impact risks of various driving variables on ecological quality changes along the Xining–Jianghe railway are significant within different spatial partitions (as shown in Figure 15). In this context, "Y" indicates the presence of significant differences, and "N" indicates no significant differences. It is observed that there are significant differences in the impact of various driving variables on ecological quality change between their different spatial partitions. The differences in the impact of annual average temperature across its various partitions on ecological quality changes are the most significant, followed by human activity intensity and annual average precipitation. There is a certain degree of spatial similarity in the impact of different land use types and altitude areas on ecological quality changes.

3.3.4. Interactive Detection and Ecological Detection Analysis of Spatial Variations in Ecological Quality among Various Factors

The study applies an interactive detector model to each driving variable, calculating Q values that represent the degree of impact on spatial variations in ecological quality resulting from the interactions between these variables. The results of these calculations are shown in Figure 16a. In the analysis of the interactive effects of various driving variables within the Xining to Jianghe railway region, the interactions after considering Q values manifested as either bilateral enhancement or nonlinear enhancement. There were no instances of variables acting independently or having a weakening effect. It was observed that the Q values significantly increased after the interaction of different driving variables. Specifically, the interactions between precipitation and land use type, human activity and precipitation, as well as human activity and temperature, led to a significant increase in the impact on regional ecological quality changes, with individual variable Q values of 0.15 increasing to approximately 0.35. However, the interaction effect of elevation with other driving factors in this region was relatively smaller. The predominant mode of interaction among these driving factors was nonlinear enhancement, further highlighting the complexity of the influences of these factors on the process of ecological quality change.

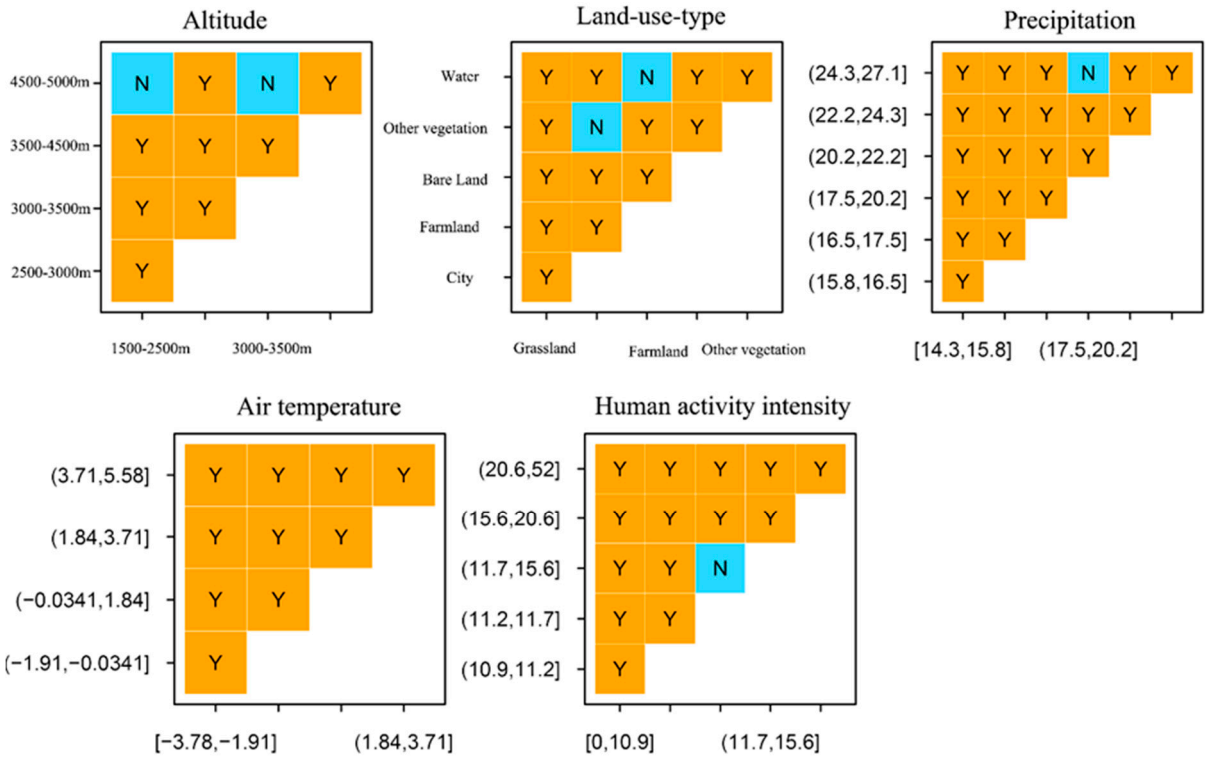

Figure 15. Distribution of the significance of driving risk of ecological quality changes by various driving variables.

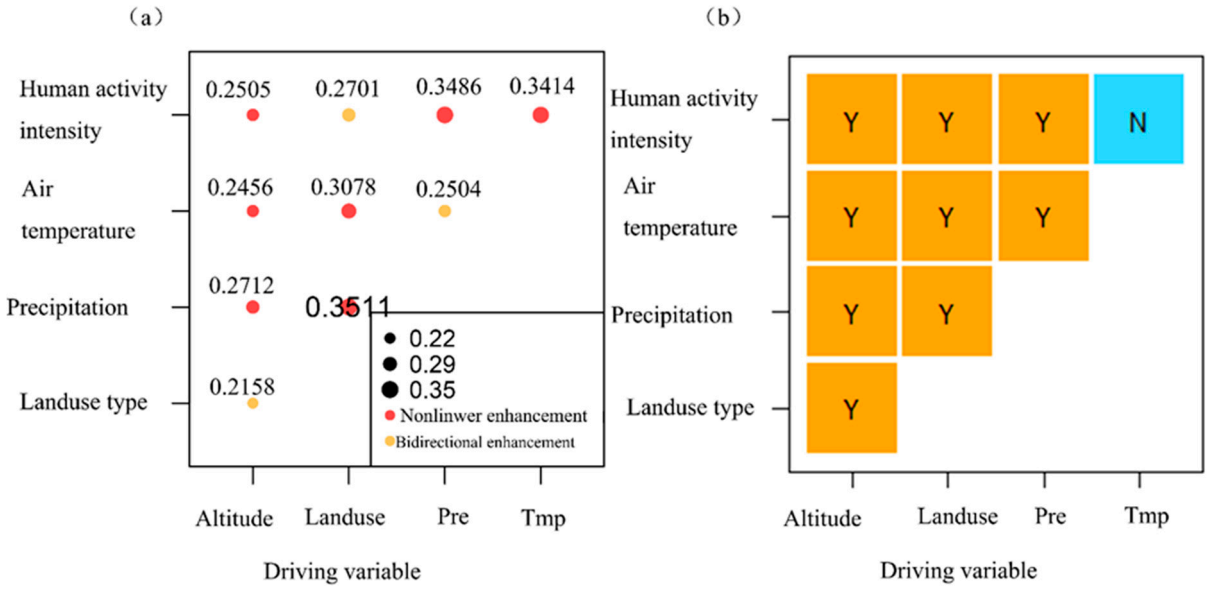

Figure 16. (**a**,**b**) Statistical results of interactive detection of spatial change of ecological quality among various factors.

Although the interaction of different explanatory variables enhances their driving effect on ecological quality change, there are still certain differences in the impact of each driving variable on ecological quality. To clarify the extent of these differences, this study further employs an ecological detection model, using an F-statistical distribution at a 0.05 significance level, to quantify the differences in the impact of human activity intensity, temperature and precipitation, land use type, and elevation on ecological quality change. In this context, "Y" indicates significant impact, and "N" indicates nonsignificant impact, with

the statistical results shown in Figure 16b. It is observed that the differences in the impact of each driving variable on ecological quality change along the Qinghai–Tibet Railway region are overall significant, indicating strong spatial heterogeneity among these factors. However, the interaction between human activity intensity and temperature changes does not show a significant impact on ecological quality change, suggesting that these two driving variables have certain similarities in their influence on regional ecological quality.

4. Discussion

(1) The Qinghai–Tibet Railway, being the world's longest plateau railway, has its route region affected by adverse plateau meteorological conditions such as cloudiness, making it difficult to obtain large-scale, seasonally consistent, cloud-free Landsat remote sensing images. This study utilized the Google Earth Engine platform to conduct pixel-level fusion and reconstruction of the least cloudy image sets from all Landsat-Collection2 Surface Reflectance images of the same season from 1986 to 2020. It then used preprocessed Top of Atmosphere (TOA) products with a total cloud cover of less than 15% as supplementary data for areas where Surface Reflectance (SR) products were missing, thereby re-synthesizing the supplemented surface reflectance products. This represents a breakthrough in dynamic monitoring and analysis of the area along the Qinghai–Tibet Railway based on multiple remote sensing data sources. However, due to the unique regional environment, there are still some issues with the data quality of Landsat-TM5 before 1990 in the region. In subsequent research, it is possible to combine AVHRR data to further integrate and process data sources from 1986 to 1900, in order to enhance the precision of the analysis results.

(2) Currently, research related to the ecological environmental quality along the Qinghai–Tibet Railway region often focuses on a single parameter that characterizes the features of alpine vegetation as the characteristic indicator [22]. The RSEI constructed in this study is based on four environmental characteristics representing the natural ecological environment: greenness, wetness, dryness, and heat. It uses a nonparametric principal component synthesis method to automatically obtain principal component indicators that account for about 85% of the contribution rate from these indicators. The resulting RSEI, a comprehensive remote sensing ecological index representing ecological quality, is more objective and scientific. However, this study only selected the Xining to Jianghe section of the Qinghai–Tibet Railway. While this method demonstrates good applicability in this area, the Qinghai–Tibet Railway spans the hinterland of the Qinghai–Tibet Plateau, with a total length of 1142 km and an average altitude of over 4500 m, crossing deserts and glaciers over long distances. The overall ecological environment is complex. Therefore, this method needs further research, taking into account the characteristics of each section, to conduct an adaptive expansion exploration study suitable for the entire Qinghai–Tibet Railway.

(3) The study found that there is a strong spatial heterogeneity among different railway stations along the Qinghai–Tibet Railway region. This study conducted spatial stratification within the region based on elevation and land use type and quantitatively constructed indicators for human activity intensity, temperature, precipitation, elevation, and land use to analyze the spatiotemporal drivers of changes in ecological environmental quality within the region.

(4) Currently, there are relatively few studies specifically focusing on the multiple impact factors along the Qinghai–Tibet Railway. Existing research primarily calculates the response of regional vegetation factors to climate change and human activities based on residuals related to meteorological data. Such methods mainly involve time-series analysis. The exploration in this study holds more value for spatial variation research. However, due to the temporal limitations of the constructed driving factor indicators, this study lacks an analysis of the various influencing factors under temporal changes. Therefore, future research needs to further strengthen the exploration and analysis of

factors affecting ecological quality changes along the railway during different time periods.

5. Conclusions

Due to the adverse meteorological conditions such as frequent cloudiness in the Qinghai–Tibet Plateau area, it is challenging to obtain large-scale, cloud-free, seasonally consistent Landsat remote sensing images. In this study, the GEE platform was utilized to rapidly synthesize cloud-free images of the same seasonal phase. Four ecological environmental indicators were calculated: greenness, wetness, dryness, and heat. Using principal component analysis (PCA), RSEI was constructed to dynamically monitor and analyze the spatiotemporal changes in ecological environmental quality along the Qinghai–Tibet Railway from 1986 to 2020. Additionally, the study modeled and analyzed the spatial variability impacts of factors such as human activities and climate factors. The main conclusions are as follows:

When dealing with large study areas and challenging environmental conditions, utilizing the algorithms provided by the GEE platform can significantly enhance the efficiency of data preprocessing. This study leveraged cloud-based parallel computing to efficiently compute a 36-year time series of remote sensing ecological indices with a 30 m spatial resolution along the Qinghai–Tibet Railway. This approach has established a new and efficient platform and data foundation for large-scale ecological environmental quality monitoring in the region.

Over the course of 36 years, the average RSEI along the Xining to Jianghe section of the Qinghai–Tibet Railway exhibited fluctuating changes, showing an overall trend of improvement through different phases of railway construction and operation. Spatially, the ecological environmental quality along the railway predominantly ranged from moderate to good. However, there were noticeable spatial differences in ecological quality around different station areas. Generally, areas closer to the train stations tended to have poorer ecological quality. Notably, the areas around Xining and Qinghai Lake stations, influenced mainly by urban and tourism development, remained in a relatively poor ecological state over an extended period.

From 1986 to 1994, following the commencement of the first phase of the railway in 1984, the ecological quality along the Qinghai–Tibet Railway began to recover from a relatively poor state. By 2002, approximately 60% of the area experienced a mild improvement in ecological quality. However, during the second phase of railway construction from 2002 to 2007, the ecological environment underwent some fluctuations, with an increase in the area experiencing mild deterioration. From 2007 to 2020, the ecological environmental quality tended to stabilize and improve, although areas close to railway stations along the line and some parts of the Xining urban area remained in a deteriorated ecological state, aligning with the research conclusions.

The impacts of various driving variables on ecological quality changes within the Qinghai–Tibet Railway region are overall significant, with strong spatial heterogeneity among different factors. There is also a degree of similarity in the impact on ecological quality among different factors, such as temperature and human activity intensity. Land use type and human activity intensity, as single factors, have the highest impact values. There are significant potential impacts on ecological environmental quality among different spatial areas, as well as interactive effects among multiple driving factors. In the study area, these interactions are manifested as either bilateral enhancement or nonlinear enhancement.

Author Contributions: Conceptualization, F.Z. and Q.H.; methodology, F.Z.; software, F.Z. and Y.L. (Yichuan Liu); validation, H.L. and X.Z.; formal analysis, Y.L. (Yuqi Liu); investigation, F.Z.; resources, F.Z.; data curation, F.Z.; writing—review and editing, Q.H.; visualization, F.Z.; supervision, F.Z.; project administration, Y.L. (Yichuan Liu); funding acquisition, F.Z. All authors have read and agreed to the published version of the manuscript.

Funding: This research was funded by Shandong Province Natural Science Foundation youth project in China, grant number ZR2023QD161.

Data Availability Statement: The data presented in this study are available on request from the corresponding author. The data are not publicly available due to privacy.

Conflicts of Interest: The funders had no role in the design of the study; in the collection, analyses, or interpretation of data; in the writing of the manuscript; or in the decision to publish the results.

References

1. Niu, F.; Gao, Z.; Lin, Z.; Luo, J.; Fan, X. Vegetation influence on the soil hydrological regime in permafrost regions of the Qinghai-Tibet Plateau, China. *Geoderma* **2019**, *354*, 113892. [CrossRef]
2. Wang, G.; Gillespie, A.R.; Liang, S.; Mushkin, A.; Wu, Q. Effect of the Qinghai–Tibet Railway on vegetation abundance. *Int. J. Remote Sens.* **2015**, *36*, 5222–5238. [CrossRef]
3. Li, Y.; Zhou, J.; Wu, X. Effects of the construction of Qinghai-Tibet railway on the vegetation ecosystem and eco-resilience. *Geogr. Res.* **2017**, *11*, 105–116.
4. Tibet Autonomous Region Railway Construction and Operation Leading Group Office Tibet Autonomous Region Development and Reform Commission. Qinghai—Tibet railway operation ten years to boost Tibet's economic and social development report. *China Railw.* **2016**, *5*, 5.
5. Sun, B.; Yang, L.; Liu, Q.; Xu, X. Numerical modelling for crushed rock layer thickness of highway embankments in permafrost regions of the Qinghai–Tibet Plateau. *Eng. Geol.* **2010**, *114*, 181–190. [CrossRef]
6. Luo, J.; Niu, F.; Liu, M.; Lin, Z.; Yin, G. Field experimental study on long-term cooling and deformation characteristics of crushed-rock revetment embankment at the Qinghai–Tibet Railway. *Appl. Therm. Eng.* **2018**, *139*, 256–263. [CrossRef]
7. Wang, L.; Wu, Z.; Sun, J.; Liu, X.; Wang, Z. Characteristics of ground motion at permafrost sites along the Qinghai-Tibet railway. *Soil. Dyn. Earthq. Eng.* **2009**, *29*, 974–981. [CrossRef]
8. Zhang, H.; Wang, Z.; Zhang, Y.; Hu, Z. The effects of the Qinghai–Tibet railway on heavy metals enrichment in soils. *Sci. Total. Environ.* **2012**, *439*, 240–248. [CrossRef] [PubMed]
9. Wu, J.; Duan, D.; Lu, J.; Luo, Y.; Wen, X.; Guo, X.; Boman, B.J. Inorganic pollution around the Qinghai-Tibet Plateau: An overview of the current observations. *Sci. Total. Environ.* **2016**, *550*, 628–636. [CrossRef]
10. Wu, Q.; Liu, Y.; Hu, Z. The thermal effect of differential solar exposure on embankments along the Qinghai–Tibet Railway. *Cold Reg. Sci. Technol.* **2011**, *66*, 30–38. [CrossRef]
11. Li, S.; Wang, C.; Xu, X.; Shi, L.; Yin, N. Experimental and statistical studies on the thermal properties of frozen clay in Qinghai-Tibet Plateau. *Appl. Clay Sci.* **2019**, *177*, 1–11. [CrossRef]
12. Zhang, M.; Wang, J.; Lai, Y. Hydro-thermal boundary conditions at different underlying surfaces in a permafrost region of the Qinghai-Tibet Plateau. *Sci. Total. Environ.* **2019**, *670*, 1190–1203. [CrossRef]
13. Wang, W.; Wu, T.; Chen, Y.; Li, R.; Xie, C.; Qiao, Y.; Zhu, X.; Hao, J.; Ni, J. Spatial variations and controlling factors of ground ice isotopes in permafrost areas of the central Qinghai-Tibet Plateau. *Sci. Total Environ.* **2019**, *688*, 542–554. [CrossRef]
14. Wu, Q.; Zhang, T.; Liu, Y. Permafrost temperatures and thickness on the Qinghai-Tibet Plateau. *Glob. Planet. Chang.* **2010**, *72*, 32–38. [CrossRef]
15. Chen, F.; Lin, H.; Li, Z.; Chen, Q.; Zhou, J. Interaction between permafrost and infrastructure along the Qinghai–Tibet Railway detected via jointly analysis of C-and L-band small baseline SAR interferometry. *Remote Sens. Environ.* **2012**, *123*, 532–540. [CrossRef]
16. Zhang, K.; Qu, J.; Han, Q.; An, Z. Wind energy environments and aeolian sand characteristics along the Qinghai–Tibet Railway, China. *Sediment. Geol.* **2012**, *273–274*, 91–96. [CrossRef]
17. Luo, L.; Duan, Q.; Wang, L.; Zhao, W.; Zhuang, Y. Increased human pressures on the alpine ecosystem along the Qinghai-Tibet Railway. *Reg. Environ. Chang.* **2020**, *20*, 33. [CrossRef]
18. Su, M.M.; Wall, G. The Qinghai–Tibet railway and Tibetan tourism: Travelers' perspectives. *Tour. Manag.* **2009**, *30*, 650–657. [CrossRef]
19. Zhao, X. Analysis of Vegetation Coverage Changes on Alpine Grassland along the Qinghai-Tibet Railway based on Remote Sensing Images—A Case Study of Wudaoliang Area. Ph.D. Thesis, China University of Geosciences, Beijing, China, 2015.
20. Zhang, L.; Miao, Y.; Wei, H.; Dai, T. Ecological Impacts Associated with the Qinghai–Tibet Railway and Its Influencing Factors: A Comparison Study on Diversified Research Units. *Int. J. Environ. Res. Public. Health* **2023**, *20*, 4154. [CrossRef] [PubMed]
21. Gao, D.; Li, S. Spatiotemporal impact of railway network in the Qinghai-Tibet Plateau on accessibility and economic linkages during 1984–2030. *J. Transp. Geogr.* **2022**, *100*, 103332. [CrossRef]
22. Chen, H.; Li, S.; Zheng, D. Features of ecosystems alongside Qinghai-Xizang highway and railway and the impacts of road construction on them. *J. Mt. Sci.* **2003**, *21*, 559–567.
23. Ding, M.J.; Shen, Z.X.; Zhang, Y.L.; Liu, L.S.; Zhang, W.; Wang, Z.F.; Bai, W.Q. Vegetation change along the Qinghai-Xizang highway and railway from 1981 to 2001. *Resour. Sci.* **2005**, *27*, 128–133.
24. Ding, M.; Zhang, Y.; Shen, Z.; Liu, L.; Zhang, W.; Wang, Z.; Bai, W.; Zheng, D. Land cover change along the Qinghai-Tibet Highway and Railway from 1981 to 2001. *J. Geogr. Sci.* **2006**, *16*, 387–395. [CrossRef]

25. Yuqing, Z. Negative impact of Qinghai-Tibetan railway construction on ecological environment of Qinghai-Tibetan Plateau. *Bull. Soil. Water Conserv.* **2002**, *22*, 50–53.
26. Luo, L.; Ma, W.; Zhuang, Y.; Zhang, Y.; Yi, S.; Xu, J.; Long, Y.; Ma, D.; Zhang, Z. The impacts of climate change and human activities on alpine vegetation and permafrost in the Qinghai-Tibet Engineering Corridor. *Ecol. Indic.* **2018**, *93*, 24–35. [CrossRef]
27. Jia, K.; Liang, S.; Wei, X.; Yao, Y.; Yang, L.; Zhang, X.; Liu, D. Validation of Global LAnd Surface Satellite (GLASS) fractional vegetation cover product from MODIS data in an agricultural region. *Remote Sens. Lett.* **2018**, *9*, 847–856. [CrossRef]
28. Huang, S.; Tang, L.; Hupy, J.P.; Wang, Y.; Shao, G.F. A commentary review on the use of normalized difference vegetation index (NDVI) in the era of popular remote sensing. *J. For. Res.* **2021**, *32*, 1–6. [CrossRef]
29. Zhang, H.; Song, J.Y.; Li, M.; Han, W.H. Eco-environmental quality assessment and cause analysis of Qilian Mountain National Park based on GEE. *Chin. J. Ecol.* **2021**, *40*, 1883–1894.
30. Gupta, K.; Kumar, P.; Pathan, S.K.; Sharma, K.P. Urban Neighborhood Green Index—A measure of green spaces in urban areas. *Landsc. Urban Plan.* **2012**, *105*, 325–335. [CrossRef]
31. Zhu, Z.; Qiu, S.; Ye, S. Remote sensing of land change: A multifaceted perspective. *Remote Sens. Environ.* **2022**, *282*, 113266. [CrossRef]
32. Ochoa-Gaona, S.; Kampichler, C.; de Jong, B.; Hernández, S.; Geissen, V.; Huerta, E. A multi-criterion index for the evaluation of local tropical forest conditions in Mexico. *For. Ecol. Manag.* **2010**, *260*, 618–627. [CrossRef]
33. Xu, H. Establishment and application of urban remote sensing ecological index. *Acta Ecol. Sin.* **2013**, *33*, 7853–7862.
34. Xu, H.; Wang, M.; Shi, T.; Guan, H.; Fang, C.; Lin, Z. Prediction of ecological effects of potential population and impervious surface increases using a remote sensing based ecological index (RSEI). *Ecol. Indic.* **2018**, *93*, 730–740. [CrossRef]
35. Yuan, F.; Bauer, M.E. Comparison of impervious surface area and normalized difference vegetation index as indicators of surface urban heat island effects in Landsat imagery. *Remote Sens. Environ.* **2006**, *106*, 375–386. [CrossRef]
36. Nichol, J. Remote Sensing of Urban Heat Islands by Day and Night. *Photogramm. Eng. Remote Sens.* **2005**, *71*, 613–621. [CrossRef]
37. Zheng, Z.; Wu, Z.; Chen, Y.; Yang, Z.; Marinello, F. Analyzing the ecological environment and urbanization characteristics of the Yangtze River Delta Urban Agglomeration based on Google Earth Engine. *Acta Ecol. Sin.* **2021**, *41*, 717–729.
38. Hu, X.; Xu, H. A new remote sensing index for assessing the spatial heterogeneity in urban ecological quality: A case from Fuzhou City, China. *Ecol. Indic.* **2018**, *89*, 11–21. [CrossRef]
39. Tao, Z.; Hong, T. Vegetation Cover Change and Urban Expansion in Beijing-Tianjin-Hebei during 2001~2015 based on Google Earth Engine. *Remote Sens. Technol. Appl.* **2018**, *33*, 593–599.
40. Mateo-García, G.; Gómez-Chova, L.; Amorós-López, J.; Muñoz-Marí, J.; Camps-Valls, G. Multitemporal Cloud Masking in the Google Earth Engine. *Remote Sens.* **2018**, *10*, 1079. [CrossRef]
41. Tsai, Y.H.; Stow, D.; Chen, H.L.; Lewison, R.; An, L.; Shi, L. Mapping Vegetation and Land Use Types in Fanjingshan National Nature Reserve Using Google Earth Engine. *Remote Sens.* **2018**, *10*, 927. [CrossRef]
42. Zurqani, H.A.; Post, C.J.; Mikhailova, E.A.; Schlautman, M.A.; Sharp, J.L. Geospatial analysis of land use change in the Savannah River Basin using Google Earth Engine. *Int. J. Appl. Earth Obs. Geoinf.* **2018**, *69*, 175–185. [CrossRef]
43. Liu, X.; Hu, G.; Chen, Y.; Li, X.; Xu, X.; Li, S.; Pei, F.; Wang, S. High-resolution multi-temporal mapping of global urban land using Landsat images based on the Google Earth Engine Platform. *Remote Sens. Environ.* **2018**, *209*, 227–239. [CrossRef]
44. Yang, X.; Wu, J.J.; Yan, F.; Zhang, J. Assessment of regional soil moisture status based on characteristics of surface temperature/vegetation index space. *Acta Ecol. Sin.* **2009**, *29*, 1205–1216.
45. Song, Y.; Wang, J.; Ge, Y.; Xu, C. An optimal parameters-based geographical detector model enhances geographic characteristics of explanatory variables for spatial heterogeneity analysis: Cases with different types of spatial data. *GISci. Remote Sens.* **2020**, *57*, 593–610. [CrossRef]
46. Wang, J.-F.; Zhang, T.-L.; Fu, B.-J. A measure of spatial stratified heterogeneity. *Ecol. Indic.* **2016**, *67*, 250–256. [CrossRef]